DEET Olfactory Reception in the Yellow Fever Mosquito

Xin Wang[1,2]†, Ru Yan[3]†, Dylan J. Brown[1]†, Qian Qi[2]†, Xuechun Feng[1,4], Zhou Chen[1], Yanjie Wang[5], Yifan Wang[1], Simin Liang[2], Heng Zhang[2], Mengli Chen[6], Yinliang Wang[7], Walter S. Leal[8*], Feng Liu[2,9*], and Nannan Liu[1*]

Affiliations:

[1]Department of Entomology and Plant Pathology, Auburn University, Auburn, USA
[2]Institute of Infectious Diseases, Shenzhen Bay Laboratory, Shenzhen, China
[3]College of Life Sciences, Zhejiang Chinese Medical University, Hangzhou
[4]School of Agriculture and Biotechnology, Zhejiang University, Hangzhou, China
[5]Genomics core, Biomedical Research Core Facilities, Shenzhen Bay Laboratory, Shenzhen, China
[6]College of Advanced Agricultural Sciences, Zhejiang A&F University, Hangzhou, China
[7]Agriculture Gene Engineering Research Center of the Ministry of Education, Northeast Normal University, Changchun 130024, China
[8]Department of Molecular and Cellular Biology, University of California-Davis, Davis, CA, USA
[9]Guangdong Provincial Key Laboratory of Infection Immunity and Inflammation, Shenzhen, China

†These authors contributed equally to this work
*Co-corresponding authors. Email: N.L. (liunann@auburn.edu); F.L. (liufeng@szbl.ac.cn), W.S.L (wsleal@ucdavis.edu)

Abstract

Developed almost 80 years ago, DEET is the first line of defense against the transmission of vector-borne diseases, and yet its mode of action is still a matter of controversy. Here we identified a dedicated odorant receptor that underlies DEET's detection as a spatial repellency for the yellow fever mosquito *Aedes aegypti*. Using heterologous expression systems, we show that this receptor is finely tuned to DEET. CRISPR-mediated disruption impaired DEET-evoked neural activity in a defined olfactory sensillum and markedly reduced spatial avoidance at behaviorally relevant concentrations. Fluorescence-guided single-sensillum recordings revealed that DEET selectively activates a distinct olfactory sensory neuron population that projects to a single, defined glomerulus in the antennal lobe, establishing a direct receptor-to-circuit link for repellency coding. These findings uncover a dedicated sensory pathway for volatile repellent detection, revealing an unexpected specialization for a manmade chemical and providing a mechanistic framework for receptor-guided development of next-generation spatial repellents.

Keywords: *Aedes aegypti*; DEET; Odorant Receptor, *AaegOr54*; Olfaction; Spatial Repellency

Introduction

Spatial repellents are a cornerstone of personal protection against insect-borne diseases, yet how volatile repellents are detected by the nervous system of the yellow fever mosquito, *Aedes aegypti*, and translated into avoidance behavior remains a matter of intense debate. In insects, host-seeking and avoidance behaviors are mediated primarily by the olfactory system, in which chemical cues are detected by three major families of ligand-gated ion channels[1], odorant receptors (Ors), ionotropic receptors (Irs), and gustatory receptors (Grs), expressed in peripheral sensory appendages[2-5]. Ors function as heteromeric complexes composed of a highly conserved co-receptor (Orco) and a ligand-selective tuning receptor (Or), with Or subunits conferring odor specificity and Orco acting as a non-ligand-binding scaffold [6,7]. Identifying the specific tuning receptors that encode ecologically relevant cues is therefore essential for understanding how olfactory systems drive adaptive behavior. N,N-diethyl-meta-toluamide (DEET) is the most widely used insect repellent worldwide and has remained the gold standard for more than 70 years[8,9].

Formulations containing 10–35% DEET provide substantial and durable protection, with efficacy increasing and plateauing near 50% DEET[10,11]. Despite occasional adverse reactions[12-14], DEET continues to be recommended by public health agencies as a primary tool for preventing vector-borne disease[15-17]. Despite its widespread use, the molecular basis of DEET's volatile (spatial) repellency remains unresolved. Competing hypotheses propose that DEET may directly activate specific odorant receptors, suppress host-odor detection, and/or disrupt the spatial structure of human odor plumes[18-20]. Volatile DEET elicits antennal responses in some mosquito lineages but not others[21-23], highlighting fundamental differences in chemosensory physiology. In *Culex quinquefasciatus*, the odorant receptor *CquiOr136* responds to DEET [24]; however, this receptor is restricted to the *Culex* lineage and is absent in *Aedes*. Thus, the molecular receptor responsible for volatile DEET detection in *Aedes aegypti* has remained unknown. Moreover, *Aedes* Orco mutants lack antennal responses to volatile DEET[22], implicating the Or pathway while leaving the identity of the tuning receptor unresolved. This gap has limited the mechanistic understanding of spatial repellency and constrained rational repellent design.

Here, we identified the molecular basis of volatile DEET detection in the mosquito *Aedes aegypti*, a globally invasive species and major vector of dengue, Zika, chikungunya, and yellow fever viruses[25]. Using single-sensillum recordings, ultra-low-input RNA transcriptomics, CRISPR-mediated gene disruption, and behavioral assays, we mapped DEET-sensitive olfactory sensory neurons to a defined trichoid sensillum subtype and identify the tuning receptor they express, *AaegOr54*. This receptor defines a dedicated DEET-sensing pathway that links peripheral detection to a single antennal-lobe glomerulus and to spatial avoidance behavior. Together, these findings resolve a long-standing question in insect chemosensation and establish a

receptor-to-circuit framework for receptor-guided development of next-generation spatial repellents.

Results

Identification of DEET-sensitive OSN in *Ae. aegypti*

To evaluate the spatial repellency of DEET, we first performed the WHO-recommended assay[26] (Fig. 1a). Low concentration of DEET (0.1%) elicited minimal repellency, whereas concentrations ≥1% produced robust and dose-dependent avoidance (Fig. 1b). We next assessed behavioral repellency in the presence of human odor cues using the hand-in-cage assay (Fig. 1c). Quantification of mosquito landing events revealed a strong dose-dependent inhibition, with higher DEET concentrations producing near-complete suppression of landings (Fig. 1d). At concentrations above 1%, DEET eliminated >99% of landing events (Extended Data Fig. S1a), confirming potent spatial repellency in *Ae. aegypti*.

To determine whether mosquito antenna detected volatile DEET, we recorded antennal responses using electroantennography (EAG) (Fig. 1e). DEET elicited clear, concentration-dependent EAG signals, with higher doses producing significantly stronger responses (Fig. 1f-1g). These findings indicated that DEET is detected by the olfactory sensilla on the mosquito antenna, which comprise several morphologically distinct types, such as trichoid, basiconic, and ceoloconic sensilla [27]. Because previous studies suggested that trichoid sensilla were preferentially activated by DEET [23,28-30], we systematically screened trichoid sensilla across all antennal flagella to identify DEET-sensitive neurons using single sensillum recording (SSR) (Fig. 1h).

Across >200 individual recordings spanning all 13 antennal flagellomeres, we identified a DEET-sensitive short sharp-tipped (SST) trichoid sensillum, which contains two olfactory sensory neurons (OSNs) distinguished by spike amplitude (Fig. 1i and Extended Data Fig. S1b). Spike-sorting analysis demonstrated that DEET exclusively activated the larger-amplitude "A" neuron. Notably, the DEET-sensitive SST sensilla were restricted to the distal four flagellomeres (10^{th}-13^{th}) and none were detected on proximal segments (1^{st} -9^{th}), indicating a spatially biased distribution along the antenna. A subsequent survey of SST sensilla within the distal flagellomeres using a panel of 28 odorants spanning multiple chemical classes revealed that SST sensilla can be classified into five functional subtypes, of which one subtype (SST-1) exhibited strong and dose-dependent activation by DEET (Fig. 1j and Extended Data Fig. S1c-d, S2). Together, these results demonstrate that DEET is detected by a dedicated OSN, the "A" neuron of the SST-1 trichoid sensillum, located specifically within the distal portion of the *Ae. aegypti* antenna.

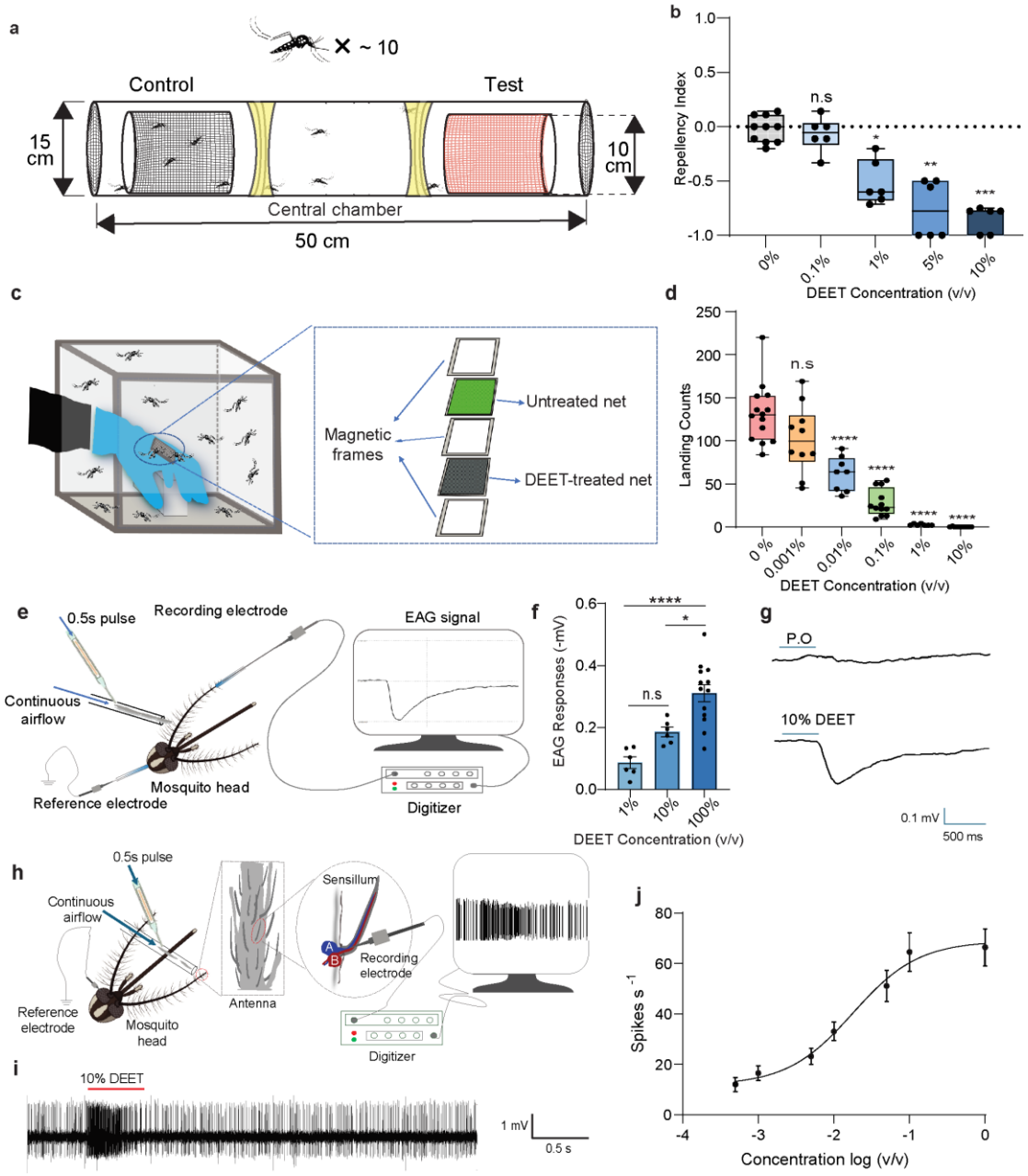

Fig. 1. DEET elicits robust spatial repellency and activates antennal olfactory neurons in *Ae. aegypti*. a, Schematic of the uniport olfactometer used to measure non-contact spatial repellency. The inner cylinders were covered with nylon treated with solvent or varying concentrations of DEET to facilitate odor release. **b,** Dose-dependent DEET repellency index in wild-type (WT) mosquitoes (n = 6-10; Kruskal–Wallis test followed by Dunn's multiple comparisons; ns, not significant; *0.01 < P < 0.05; **0.001 < P < 0.01; ***0.0001 < P < 0.001). **c,** Schematic of the hand-in-cage assay. **d,** Effect of DEET concentration on mosquito landing counts (n = 8-14; Kruskal-Wallis test with Dunn's multiple comparisons; ns, not significant; ****P < 0.0001). **e,** Schematic of electroantennogram (EAG) setup. **f,** Concentration-dependent EAG responses to DEET (n = 6-12; Kruskal-Wallis test with Dunn's multiple comparisons; ns, not significant; ****P < 0.0001). **g,** Representative EAG traces from WT antennae stimulated with solvent (paraffin oil, P.O.) and DEET

(10%). **h,** Schematic of the single sensillum recording (SSR) setup. **i,** Representative SSR traces from an SST-1 sensillum showing strong activation of the "A" neuron by DEET (10^{-1} v/v). **j,** Dose-dependent SSR responses to DEET in WT mosquitoes (n = 10-12).

Identification of odorant receptors expressed in the DEET-sensitive neurons

Previous studies demonstrated that DEET reception in mosquitoes is mediated by the Or/Orco complex[31], and loss of the *Orco* gene abolishes DEET-evoked behavioral repellency in *Ae. aegypti*[22]. We therefore sought to identify the specific odorant receptor(s) expressed in the DEET-sensitive SST-1 "A" neurons of *Ae. aegypti*. After confirming that DEET-responsive SST-1 sensilla are restricted to the distal four flagellomeres (10^{th}–13^{th}) of the antenna (Fig. 2a), we microdissected individual antennae across 3 biological replicates into proximal (1^{st}–9^{th}) and distal (10^{th}–13^{th}) regions for comparative transcriptomic profiling using ultra-low-input RNA sequencing, a method capable of detecting transcripts from only a few antennal flagellomeres.

Because electrophysiological mapping localized DEET-responsive OSNs exclusively to the distal region, we reasoned that candidate DEET receptors would be highly enriched distally but minimally expressed proximally. Candidate genes were therefore selected using two stringent criteria: (1) very low expression levels (TPM < 1) in the proximal region, and (2) significantly higher expression in the distal region. Of the 91 *Ae. aegypti* Or genes detected, seven (*AaegOr20, AaegOr25, AaegOr31, AaegOr33, AaegOr54, AaegOr55, and AaegOr57*) met both criteria (Fig. 2b and Extended Data Fig. S3a, Table S1)**.** Among these, *AaegOr54* and *AaegOr55* share 87.66% amino acid sequence identity.

To test whether any of these receptors respond to DEET, we amplified their coding sequences from antennal cDNA and co-expressed each with *Ae. aegypti* Orco (*AaegOrco*) in *Xenopus laevis* oocytes (Fig. 2c). Two-electrode voltage clamp recordings revealed that only *AaegOr54/Orco* and *AaegOr55*/*Orco* heteromeric complexes generated significant inward currents in response to DEET, with amplitudes of 1,462 ± 155 nA (n = 5) and 345 ± 28 nA (n = 6), respectively (Fig. 2d and Extended Data Fig. S3b-c). Dose-response analyses showed that *AaegOr54* is substantially more sensitive to DEET ($EC_{50} = 2.16 \times 10^{-5}$ M) than *AaegOr55* ($EC_{50} = 4.94 \times 10^{-4}$ M) (Fig. 2e), indicating a predominant role for *AaegOr54* in detecting DEET.

We next focused on *AaegOr54* and examined its tuning breadth using a panel of structurally diverse odorants. In *the Xenopus* oocyte expression system, *AaegOr54*/Orco displayed striking selectivity, responding almost strongly to DEET, with a high kurtosis value (K = 114.6) (Fig. 2f and Extended Data Table S2). To evaluate *AaegOr54* function in a neuronal context, we expressed *AaegOr54* using the *Drosophila melanogaster* 'empty' neuron system (Fig. 2g), in which the *Or22*a/b genes are deleted[32]. Expression of *AaegOr54* conferred strong and dose-dependent responses to DEET across a panel of 186 compounds, and DEET elicited the strongest activation among all tested odorants (Fig. 2h-i and Extended Data S3d-e, Table S3). Although its tuning profile was broader in this neuronal platform than in *the Xenopus oocyte* expression system, the magnitude and specificity of DEET activation remained highest. Together with TEVC recordings, these results identify *AaegOr54* and *AaegOr55* as DEET-responsive receptors, with *AaegOr54* exhibiting exceptionally high sensitivity, making it the strongest mediator of volatile DEET detection in *Ae. aegypti*.

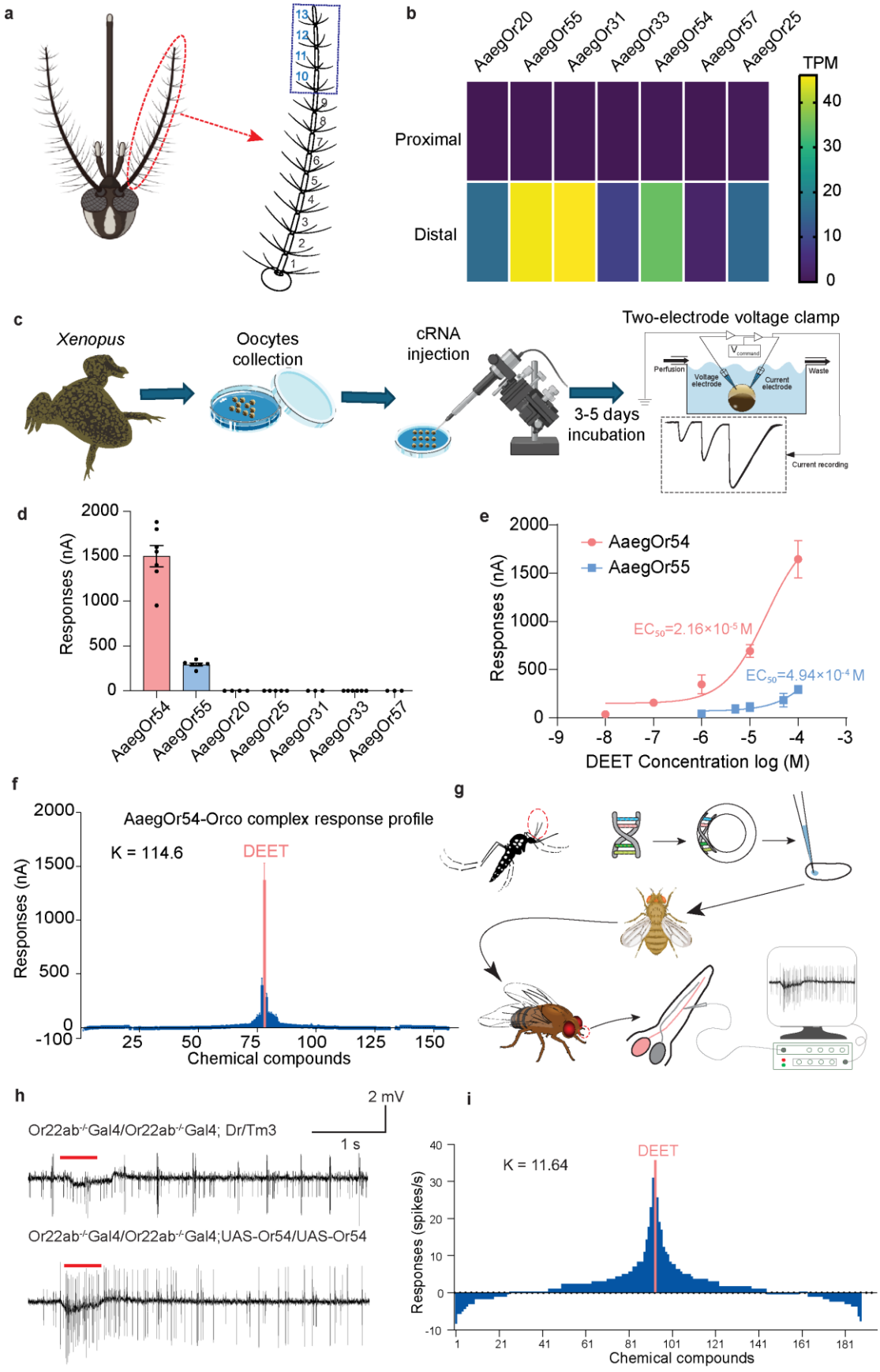

Fig. 2. Identification of *AaegOr54* as the DEET receptor in *Ae. aegypti*. a, Image of the *Ae. aegypti* antenna. The numbers indicate flagellomeres from the antennal base

(1^{st}) to the tip (13^{th}). Flagellomeres 1-9 constitute the proximal region, whereas 10^{th}-13^{th} form the distal region. **b,** Heatmap showing the average transcript levels of seven candidate AaegOrs that met the selection criteria (n = 3). The dark blue-green-yellow color gradient indicates expression levels, ranging from low (dark blue) to high (yellow) **c,** Schematic of the *Xenopus laevis* oocyte expression system. **d,** Responses of the seven candidate AaegOrs to DEET (10^{-4} M). **e,** Dose-response curves of *AaegOr54* and *AaegOr55* to DEET. EC_{50} of *AaegOr54* = 2.16×10^{-5} M; EC_{50} of *AaegOr55* = 4.94×10^{-4} M. **f,** Tuning curve of *AaegOr54* (n = 3-9). Tested compounds are arranged along the x-axis, with those eliciting the strongest responses near the center and weaker ligands toward the edges. The kurtosis (k), indicating tuning "peakedness" is shown. **g,** Schematic of the *Drosophila* empty neuron expression system. **h,** Representative SSR traces from control flies (*Or22*ab$^{-/-}$-*Gal4*/*Or22*ab$^{-/-}$-*Gal4*; *Dr*/*Tm3*) and transgenic flies (*Or22*ab$^{-/-}$-*Gal4*/*Or22*ab$^{-/-}$-*Gal4*; *UAS-AaegOr54*/*UAS-AaegOr54*) in the ab3A neuron in response to DEET (10^{-2} v/v). **i,** Tuning curve of *AaegOr54* expressed in the *Drosophila* empty neuron system (n = 3). Tested compounds are arranged along the x-axis, with those eliciting the strongest responses near the center and weaker ligands toward the edges. The kurtosis (k) is shown.

AaegOr54 knockout significantly reduces electrophysiological responses to DEET

Because *AaegOr54* and *AaegOr55* showed strong and moderate DEET responses, respectively, in heterologous expression systems, we next investigated their functional roles *in vivo*. Using CRISPR/Cas9 genome editing, we generated independent loss-of-function mutants for both receptors (Fig. 3a-b and Extended Data Table S4). Homozygous *AaegOr54*$^{-/-}$ and *AaegOr55*$^{-/-}$ lines were validated by PCR amplification of the target locus followed by Sanger sequencing. Electroantennogram (EAG) recordings revealed a pronounced reduction in DEET-evoked antennal responses in *AaegOr54*$^{-/-}$ mutants across all tested concentrations (Fig. 3c-e). In contrast, *AaegOr55*$^{-/-}$ lines showed EAG responses indistinguishable from wild-type mosquitoes (Fig. 3c-e). These results indicate that *AaegOr54*, but not *AaegOr55*, is required for DEET-evoked antennal activation.

To determine whether *AaegOr54* knockout eliminates DEET-sensitive sensilla, we performed a comprehensive SSR survey with individual recordings of SST sensillum across the distal four flagellomeres. In wild-type mosquitoes, 10 of 70 (14.3%) SST sensilla exhibited strong DEET-evoked OSN activation (Fig. 3f, Extended Data Fig. S4). In striking contrast, none of the 88 SST sensilla recorded from *AaegOr54*$^{-/-}$ mutants showed any response to DEET (Fig. 3f, Extended Data Fig. S4). This complete loss of sensillum responsiveness confirms that the DEET-activated SST-1 "A" neuron depends entirely on functional *AaegOr54*. Together, these data demonstrate that *AaegOr54*, but not *AaegOr55*, is the essential odorant receptor mediating DEET-evoked neuronal activation in *Ae. aegypti*.

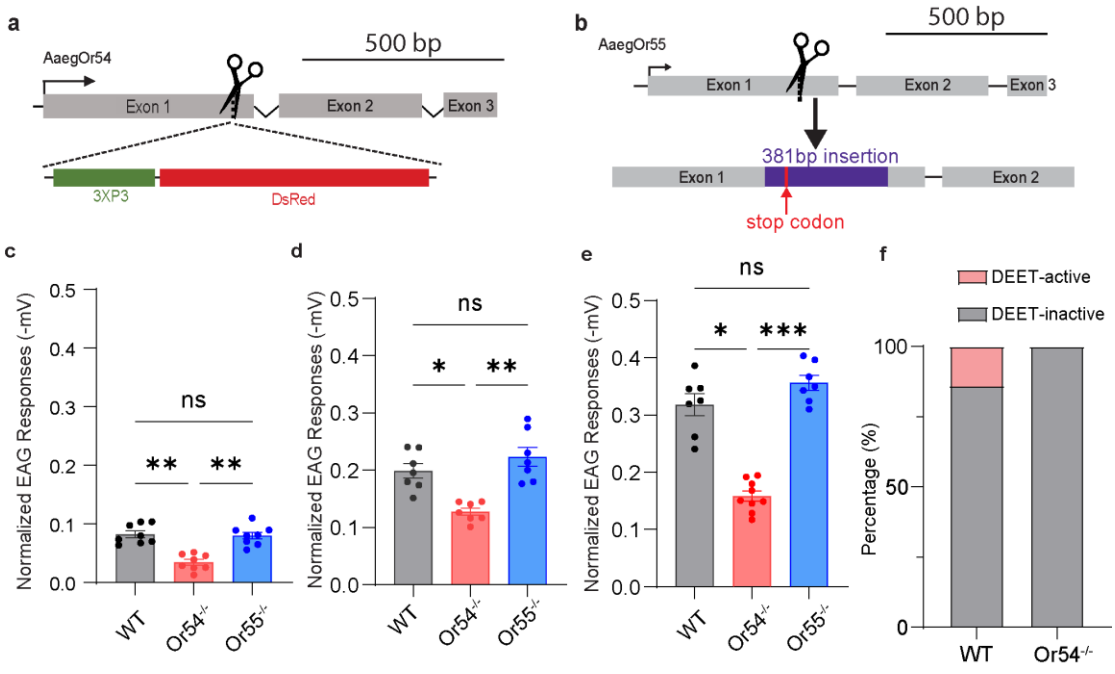

Fig. 3. *AaegOr54* mutation attenuates electrophysiological responses to DEET. a, Schematic of CRISPR/Cas9-mediated *AaegOr54* mutagenesis. **b,** Schematic of CRISPR/Cas9-mediated *AaegOr55* mutagenesis. Non-homologous end joining (NHEJ) resulted in a 381-bp insertion, the 5′ end of which contained a premature termination codon. **c-e,** DEET responses of WT, *AaegOr54* knockout (*AaegOr54*$^{-/-}$), and *AaegOr55* knockout (*AaegOr55*$^{-/-}$) mosquitoes to DEET at 1% (**c**), 10% (**d**), and 100% (**e**) (n = 7-9). The data shown in this figure represent DEET response values after subtraction of the P.O. (solvent) response. **f,** Activation rate of sensilla in WT and *AaegOr54*$^{-/-}$ antennae.

Anatomical and functional validation of *AaegOr54*-expressing neurons

To further validate the role of *AaegOr54*-expressing olfactory sensory neurons (OSNs) in DEET detection, we performed fluorescence-guided single sensillum recording (FgSSR), which integrates SSR with a binary Q-system[33] enabling visual localization of target sensilla (Fig. 4a). We generated an *AaegOr54*-QF2 driver line by inserting a *T2A-QF2-3×P3-DsRed* cassette into the first exon of *AaegOr54* (Fig. 4b and Extended Data Table S4). This knock-in produced DsRed fluorescence in the compound eyes (Extended Data Fig. S5a). When crossed to a *QUAS-mCD8:GFP*[33] reporter strain with ECFP fluorescence in the compound eyes (gift from Dr. Leslie Vosshall, Rockefeller University), the progeny (*AaegOr54*$^{+/QF2}$ > *QUAS-mCD8:GFP*) exhibited bright GFP labeling in all *AaegOr54*-expressing OSNs along with DsRed/ECFP in the eyes (Extended Data Fig. S5b). This dual-reporter system allowed unambiguous identification of sensilla housing *AaegOr54*-positive neurons.

Consistent with our ultra-low-input RNA transcript profiling, all GFP-labeled sensilla belonged to the SST subtype and were restricted to the distal four flagellomeres (10th

–13th) in females, with the highest density on the 13th flagellomere (Fig. 4c) which contains a significantly higher number of *AaegOr54*-expressing neurons (~6 neurons) compared with the remaining distal flagellomeres, which each contains approximately one neuron (Extended Data Fig. S5c). In males, GFP-labeled sensilla were restricted to the 13th flagellomere (Extended Data Fig. S5d). Immunofluorescence of the brains further revealed that all *AaegOr54*-expressing OSNs projected to a single, well-defined glomerulus in the anterior antennal lobe (Fig. 4d and Extended Data Fig. S5e). Three-dimensional reconstruction confirmed that these neurons target the AL3 glomerulus, a member of the anterolateral glomerular group (Fig. 4e-g)[34,35]. These anatomical data demonstrate that *AaegOr54* exhibits a highly localized distal antennal expression and funnels its sensory input into a single glomerulus, forming a dedicated olfactory channel.

FgSSR recordings showed that *AaegOr54*-positive SST sensilla (*AaegOr54*$^{+/QF2}$>*QUAS-mCD8:GFP*) responded strongly to DEET, with robust responses to an additional subset of compounds (Fig. 4h-i), which is well aligned with the response profile of the DEET-sensitive SST-1 sensillum in the wildtype mosquito ($r = 0.9567$) (Extended Data Fig. S5f). To compare responses between the heterologous *Drosophila* empty-neuron (ab3A) expression system and endogenous mosquito neurons, we performed a correlation analysis using response profiles obtained from both systems with the same odorant panel (FgSSR panel), which revealed a moderate correlation coefficiency ($r = 0.62$) (Extended Data Fig. S5g). .

Because insertion of the *T2A-QF2-3×P3-DsRed* cassette disrupts the endogenous *AaegOr54* coding sequence, homozygous knockout mosquitoes (*AaegOr54*$^{QF2/QF2}$ > *QUAS-mCD8:GFP*), selected by PCR verification, served simultaneously as fluorescent reporter animals and loss-of-function mutants. Recordings from these mutants showed a complete loss of DEET-evoked activity, together with strongly reduced or abolished responses to several terpenoid compounds (e.g., (-)-fenchone, α-(-)-thujone, eucalyptol) and heterocyclic/benzoic compounds (e.g., 2-acetylthiophene, 2-acetylpyridine, methyl benzoate, methyl o-toluate, benzaldehyde) (Fig. 4i and Extended Data Fig. S6). A small residual response persisted in mutant neurons, suggesting that additional chemoreceptors may be co-expressed within these OSNs. Together, these *in vivo* recordings demonstrate that *AaegOr54*-expressing SST-1 “A” neurons on the distal antenna are the primary detectors of volatile DEET in *Ae. aegypti*.

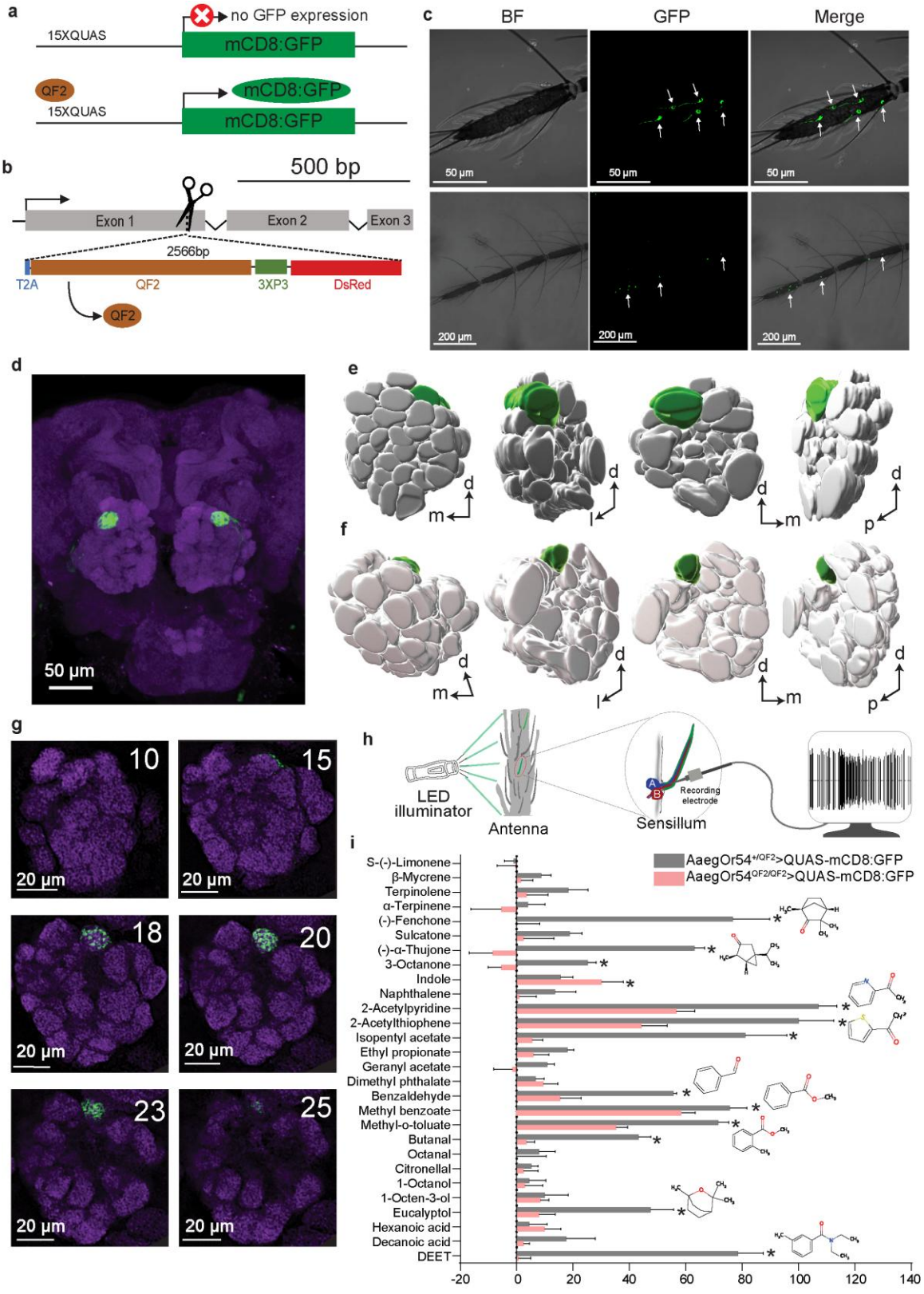

Fig. 4. Organization of *Ae. aegypti* antennal lobe glomeruli and projections of *AaegOr54-QF2*-expressing neurons. a, Schematic of the binary Q-system used to label *AaegOr54*-expressing olfactory sensory neurons (OSNs). **b,** Schematic of CRISPR-mediated insertion of the *T2A-QF2-3×P3-DsRed* cassette into the *AaegOr54* locus. **c,** Representative maximum-intensity projections of confocal z-stacks showing

GFP-labeled SST sensilla on the 13th flagellomere (top) and across the 10th-13th flagellomeres (bottom) of female antennae. Arrowheads indicate *AaegOr54*-expressing neurons. **d,** Immunofluorescent staining of the adult female antennal lobe showing GFP-positive axons of *AaegOr54*-expressing OSNs. **e-f,** Three-dimensional reconstruction of a representative right antennal lobe viewed from four angles; the *AaegOr54*-innervated glomerulus is highlighted in green. **g,** Single optical sections from the confocal z-stack shown in (**d**), with immunolabeling for GFP (green) and Brp (synaptic marker, magenta). Numbers in the upper right indicate depth relative to the glomerulus surface, illustrating spatial localization of the *AaegOr54*-targeted glomerulus. **h,** Schematic of fluorescence-guided single sensillum recording (FgSSR). **i,** Odorant response profiles of *AaegOr54*-expressing SST sensilla in heterozygous (*AaegOr54*$^{+/QF2}$ > *QUAS-mCD8:GFP*; n = 5-6) and homozygous (*AaegOr54*$^{QF2/QF2}$ > *QUAS-mCD8:GFP*; n = 6-7) lines. Responses to each compound were compared between genotypes using the nonparametric Mann–Whitney test (*P < 0.05). Representative compounds that showed significantly different responses are labeled with their chemical structures.

Reduced repellency of DEET in *AaegOr54* knockout mosquitoes

To determine whether *AaegOr54* is required for DEET-mediated spatial repellency, we evaluated avoidance behavior in *AaegOr54* knockout (*AaegOr54*$^{-/-}$) mosquitoes using two complementary paradigms: the hand-in-cage assay, which incorporates human odor cues, and the WHO spatial-repellency assay performed in the absence of human volatiles.

WHO spatial-repellency assay (odor-free conditions). To isolate the olfactory component of DEET repellency and eliminate interference from human odor plumes, we used the WHO spatial-repellency assay under odor-free conditions. Solvent controls revealed no differences between WT and *AaegOr54*$^{-/-}$ mosquitoes (Fig. 5a), indicating that the knockout exhibits normal baseline movement and decision-making in this arena. At 0.1% DEET, both genotypes showed comparable levels of repellency (Fig. 5b). In contrast, at higher concentrations (1%, 5%, and 10%), repellency was significantly reduced in *AaegOr54*$^{-/-}$ mosquitoes relative to WT (Fig. 5c-e). These results indicate that *AaegOr54* is required for robust volatile DEET avoidance under odor-free conditions. Notably, residual repellency persisted in *AaegOr54*$^{-/-}$ mosquitoes even at 10% DEET, suggesting that additional sensory pathways—such as modulation of other odorant receptors, activation of non-Or olfactory channels, or Or-independent contact chemoreception—may contribute to DEET detection at higher concentrations.

Hand-in-cage assay (with human odor cues). We examined whether deletion of *AaegOr54* affects baseline attraction to human odor. *AaegOr54*$^{-/-}$ mutants exhibited normal attraction to a human hand, comparable to wild-type (WT) controls (Extended Data Fig. S7a), confirming that *AaegOr54* does not participate in host-seeking behavior itself. DEET produced a clear dose-dependent inhibition of landing behavior

in *AaegOr54* mutants (Extended Data Fig. S7b). At very low concentrations (0.001%), neither genotype exhibited detectable repellency (Fig. 5f). However, at 0.01% and 0.1% DEET, *AaegOr54*$^{-/-}$ mutants showed significantly weaker repellency than WT (Fig. 5g-h), demonstrating that *AaegOr54* is required for detecting low concentrations of volatile DEET under realistic conditions in which host odors are present. At higher concentrations (1–10%), DEET still produced strong inhibition in both strains (Fig. 5i-j). The persistence of avoidance in the knockout strain is likely attributable to DEET's well-described non-specific masking and/or "confusant" effects on host-odor perception [36-38], which can dominate behavioral output in hand-in-cage assays and obscure the contribution of specific olfactory receptors when DEET is presented at saturating doses.

Together, these behavioral analyses establish that *AaegOr54* is essential for low- and intermediate-dose spatial repellency and is a major determinant of volatile DEET detection in *Ae. aegypti*. At higher concentrations, additional olfactory or non-olfactory pathways potentially compensate for the loss of *AaegOr54*, explaining the incomplete abolishment of avoidance behavior observed in the knockout strain.

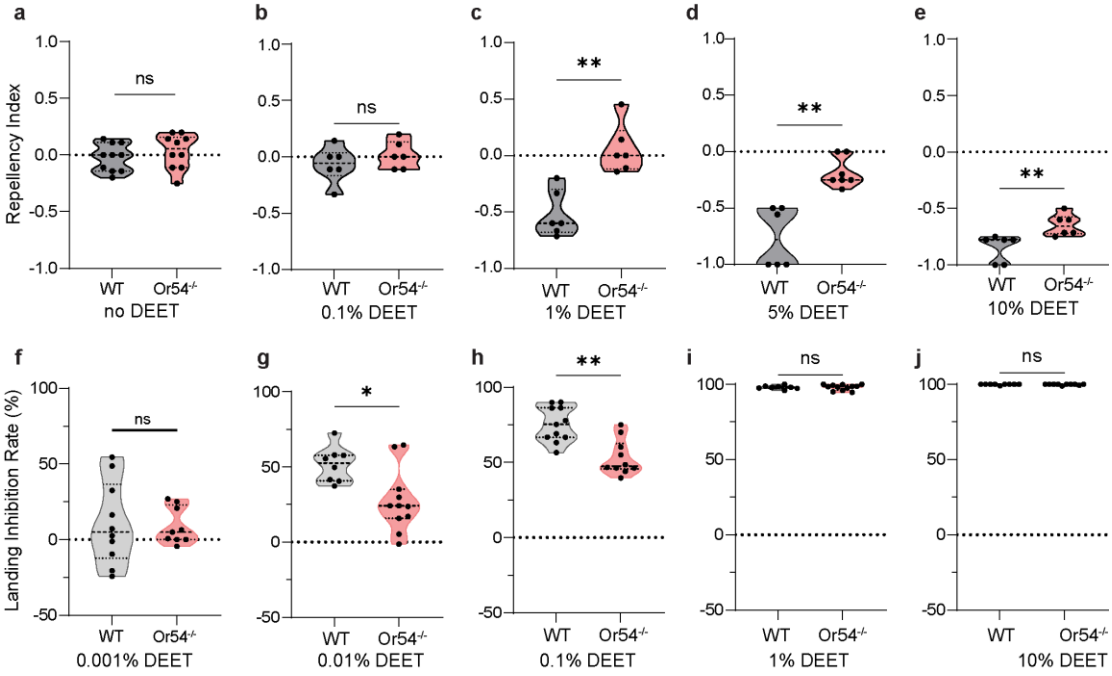

Fig. 5. *AaegOr54* knockout reduce DEET repellency in *Ae. aegypti*. a-e, Repellency indices of WT and *AaegOr54*$^{-/-}$ mosquitoes assessed using the unidirectional olfactometer at DEET concentrations of 0% (**a,** no DEET), 0.1% (**b**), 1% (**c**), 5% (**d**), and 10% (**e**) (n = 6-7). Statistical comparisons between genotypes at each concentration were performed using the Mann–Whitney test (ns, not significant; **0.001 < P < 0.01). **f-j,** Landing inhibition rates of WT and *AaegOr54*$^{-/-}$ mutant mosquitoes exposed to DEET in the hand-in-cage assay at 0.001% (**f**), 0.01% (**g**), 0.1% (**h**), 1% (**i**), and 10% (**j**) (n = 8-11). Statistical comparisons between WT and *AaegOr54*$^{-/-}$ groups were performed using the Mann–Whitney test (ns, not significant; *0.01 < P < 0.05; **0.001 < P < 0.01).

Discussion

The molecular basis of DEET repellency has been debated for decades, particularly the contribution of odorant receptors (Ors) to spatial avoidance behavior [22,28,31,39]. Previous work in *Culex quinquefasciatus* identified the receptor CquiOr136 as contributing to antennal responses and behavioral repellency to DEET and related compounds [24]. In contrast, the present study establishes a direct causal link between a single odorant receptor and spatial avoidance behavior through CRISPR-mediated disruption of *AaegOr54*, demonstrating that loss of receptor function abolishes DEET-evoked neural activity and significantly reduces repellency. Beyond this causal relationship, we define a multi-level mechanistic framework linking odor detection to behavior, integrating receptor function, in vivo neural activity, defined olfactory sensilla, and behavioral responses. We further identify the neural circuitry underlying DEET detection in *Aedes aegypti*, showing that DEET-responsive *AaegOr54*-expressing neurons arise from a specific sensillum type and project to a single, anatomically defined glomerulus. While spatial organization of olfactory sensory neurons and glomerular convergence are well-established principles, their functional implementation in a behaviorally relevant repellent pathway has not been previously resolved in mosquitoes.

Notably, the DEET-sensitive pathway identified here quite differs from that described in *Culex*. Whereas *CquiOr136* responds broadly to multiple commercial mosuqito repellents, including DEET, IR3535, Picaridin, and PMD, *AaegOr54* exhibits selective sensitivity to DEET, certain plant-derived terpenoids, aromatics and heterocyclics. These differences in ligand tuning, together with the observation that residual repellency persists in *AaegOr54* mutants, indicate that DEET detection likely involves multiple sensory pathways and that *AaegOr54* represents a key, but not exclusive, contributor to repellency. Recent single-nucleus transcriptomic studies indicate that *AaegOr54*-expressing neurons may co-express additional olfactory receptors[40,41], which could contribute to the residual odor responses observed in Or54 mutants. Collectively, these findings support the idea that DEET-sensitive odorant receptors have evolved distinct functional properties across mosquito lineages, suggesting convergent evolution in volatile repellent detection. While our findings establish a role for *AaegOr54* in DEET detection, we did not directly test whether activation of this pathway is sufficient to drive repellency, nor whether it represents the sole olfactory pathway responsive to DEET. In addition, EAG responses still can be detected in the absence of *AaegOr54*, suggesting that other receptors on the antennae are likely involved in DEET reception.

Consistent with these observations, because DEET is a compound synthesized in 1946 (about 80 years ago), it is unlikely that mosquito receptors evolved specifically for its detection. Rather, DEET may activate receptors that naturally respond to structurally

or functionally related compounds. Indeed, *in vivo* FgSSR recordings showed that *AaegOr54* is activated by a subset of naturally occurring ligands that share a conserved 'polar–apolar' structural motif, typically consisting of a carbonyl or oxygen-containing group linked to a hydrophobic ring (Fig. 4i). Many of these compounds, including (-)-fenchone, α-(-)-thujone, and eucalyptol, are major constituents of essential oils with documented repellent activity against mosquitoes [42,43]. Others, such as 2-acetylthiophene and benzaldehyde, have also been shown to elicit mosquito repellency in behavioral assays [44,45]. Although methyl benzoate has not been reported as a mosquito repellent, it is a strong repellent to other hematophagous or agricultural pests, such as bed bugs and whiteflies [46,47]. Together, these findings support the hypothesis that *AaegOr54* may have evolved to detect structurally related natural repellents, with DEET acting as a fortuitous synthetic mimic that engages a pre-existing avoidance pathway. Given the deep evolutionary divergence among mosquito genera, *Anopheles* (~150-200 million years ago) and the *Aedes*-*Culex* split (~50-100 million years ago), distinct mosquito lineages appear to have independently recruited different Ors to detect DEET and other structurally related repellents. For example, *CquiOr136* is restricted to *Culex*, and *AaegOr54* appears specific to *Aedes* mosquito, with no clear orthologs in *Anopheles*. This represents a striking case of convergent evolution in repellent detection pathways driven by ecological pressures resulting in spatial avoidance.

Although multiple mechanisms of DEET action have been proposed, work using *orco* mutants in *Ae. aegypti* has led to two principal hypotheses: (1) DEET activates specific odorant receptors that drive avoidance, and (2) DEET broadly modulates Or activity, producing a sensory “confusant” effect that disrupts host-odor perception [23,28,29,36-39]. Our findings support the specific-activation model by demonstrating that *AaegOr54* is both necessary and sufficient for detection of volatile DEET. *AaegOr54*-expressing OSNs are confined to a distinct SST-1 trichoid sensillum subtype in the distal antennal flagellomeres and project exclusively to the AL3 glomerulus, consistent with observed DEET-evoked activity in this region [48]. A previous study reported a different DEET-responsive glomerulus (AM2) in *Ae. Aegypti* [49]. The discrepancy between our identified glomerulus (AL3) and AM2 may reflect the involvement of different DEET-responsive receptors or differences in glomerular nomenclature. Moreover, DEET has been shown to activate additional antennal lobe regions (MD and PD)[48], which are likely innervated by IR76b-expressing neurons[2], suggesting that non-Or pathways may also contribute to DEET detection. It is important to note that our survey of DEET-sensitive sensilla primarily focused on SST sensilla based on prior studies, and therefore represents only a subset of the sensilla present on the mosquito antenna. Other sensillum types, such as grooved peg and coeloconic sensilla—which are known to house olfactory sensory neurons expressing ionotropic receptors (IRs)—may also contribute to the spatial detection of DEET.

The *AaegOr54* pathway, therefore, may represent a labeled-line architecture for DEET detection, distinct from the combinatorial glomerular coding typical of host-

associated odorants[48]. This organization suggests that the mosquito olfactory system treats DEET as a dedicated avoidance cue, such that activation of the AL3 glomerulus may contribute to repellency. The distal enrichment of *AaegOr54* OSNs mirrors other spatially organized chemosensory microdomains, such as the uneven distribution of ionotropic receptors in *Anopheles* antennae[50], suggesting a compartmentation-based odor coding mode in mosquito olfaction.

Of note, in heterologous expression assays, DEET was consistently the most potent agonist; however, secondary tuning profiles varied across platforms, reflecting limitations inherent to non-native receptor contexts[51,52]. In contrast, endogenous *Aedes* Or54-expressing OSNs displayed high sensitivity to DEET as well as other compounds that closely paralleled behavioral repellency, underscoring the importance of in vivo receptor context, including native Orco, accessory proteins, and membrane physiology, in defining true ligand specificity.

Genetic ablation of *AaegOr54* eliminated DEET-evoked responses in SST-1 sensilla and markedly reduced spatial repellency across low to intermediate concentrations (0.01–10%). At higher doses, DEET continued to elicit strong avoidance in both wild-type and knockout mosquitoes, consistent with masking and/or "confusant" effects on host-odor perception[21,28,31,36,38]. The use of a standardized spatial-repellency assay was critical for eliminating interference from human odor, previously shown to obscure responses to compounds such as nootkatone [26], thereby isolating the specific contribution of *AaegOr54* to volatile DEET detection. Residual repellency at 10% DEET suggests recruitment of additional mechanisms, including activation of additional ORs and/or broad OR modulation [36,53,54]. Notably, *AaegOR55* shares highly conserved amino acid sequence similarity with *AaegOr54* and exhibits weak responses to high concentrations of DEET. This similarity in amino acid sequence and DEET-evoked activation may provide useful framework for future structure-function studies to identify the regions of Ors, particularly *AaegOr54,* that mediate DEET binding. In addition, there are several additional Ors, including *AaegOr55*, found to be co-expressed within some *AaegOr54*-expressing OSNs based on the single-cell atlases generated by Goldman et al.[40] and Adavi et al.[41], which may explain the residual spikes of Or54 knockout OSNs in response to certain compounds (e.g. 2-acetylpyridine and 2-acetylthiophene), however, no residual responses elicited by DEET was observed, suggesting the predominant role of *AaegOr54* (but not other co-expressed Ors) in detecting DEET.

Conclusions and implications

Our integrated genetic, electrophysiological, and behavioral analyses establish *AaegOr54* as the central molecular determinant of volatile DEET reception in *Ae. aegypti*. To our knowledge, this is the first identification of a bona fide DEET receptor in *Aedes* mosquitoes, revealing a chemical repellent sensory pathway that links

519 peripheral OSN activation to glomerular projection and avoidance behavior.
520 *AaegOr54*'s exceptional sensitivity provide a mechanistic foundation for rational
521 design of next-generation spatial repellents, including safer and more durable
522 compounds tailored to mosquito chemosensory biology. Receptor-guided strategies
523 offer strong potential to transform chemical vector management and reduce the global
524 burden of mosquito-borne disease.
525
526

Method

Mosquito rearing

The *Ae. aegypti* mosquitoes were maintained under controlled conditions at 27 ± 2°C, 75 ± 5% relative humidity, and a 12:12 h light:dark photoperiod. Larvae were reared in deionized water and fed TeraMin Tropical Fish Flakes according to their needs. After pupation, male and female pupae were collected and placed together in the rearing cages, where adults were provided with a 10% sucrose solution. Adult females were blood-fed using cow blood obtained from the Large Animal Teaching Hospital at Auburn University.

Hand-in-cage assay

Spatial (non-contact) repellency was evaluated using a modified hand-in-cage assay based on previous study[55]. Assays were conducted in a 30 cm × 30 cm × 30 cm mosquito cage equipped with a top-mounted digital camera connected to the computer for video recording and quantitative analysis. A nitrile glove was modified by cutting a 6 × 5 cm window on the dorsal surface. A magnetic frame, slightly larger than the opening, was affixed around the cutout to increase a stable base for stacking additional magnetic frames to a total height of approximately 10.0 mm. Two layers of polyester netting were used: a lower “chemical treated” net positioned about 3 mm above the glove surface, and an upper “untreated” net positioned roughly 8 mm above the glove. This configuration ensured that mosquitoes could land on the untreated net without physically contacting the treated one. The two nets were separated and secured by stacked magnetic frames held together with a binder clip.

Female mosquitoes (4-9 day-old, non-blood fed) were aspirated into cages in groups of approximately 40 individuals 24 hours prior to testing. A water-soaked cotton pad was placed on the cage top to maintain hydration. All assays were performed at 27-28 ºC and ~50% relative humidity. Immediately before testing, the lower net was placed in a Petri dish and treated with 500 µL of either acetone (solvent control) or a DEET solution at the desired concentration. Nets were prepared in an adjacent room, and acetone was allowed to evaporate completely (~ 7 min) before the net was assembled onto the glove. The tester then inserted gloved hand into the cage and mosquito behavior was recorded for 5 minutes. Landing events on the upper, untreated net were quantified from minute 2 through minute 5 of each trial.

Each cage was first treated with the solvent control and subsequently with the DEET treatment. A minimum interval of 90 minutes was allowed between trials to ensure full recovery of mosquitoes landing activity and to ventilate volatiles from the room. Control trials in which mosquitoes exhibited abnormally low landing activity were excluded from analysis. Percent repellency was calculated using the formula: Landing inhibition rate (%) = $(1 - N_{DEET} / N_{control}) \times 100$, where N_{DEET} is the cumulative number of landings under DEET treatment, and $N_{control}$ is the cumulative number under solvent control.

Immediately after each assay, cages were sprayed with 70% ethanol, rinsed with distilled water, sprayed again with ethanol, and allowed to airdry. The modified glove and magnetic frames were similarly decontaminated by soaking in 70% ethanol, rinsing with distilled water, and applying a final ethanol rinse before air-drying.

Uniport olfactometer assay

A modified spatial-repellency assay was used to quantify mosquito avoidance of volatile stimuli (DEET or solvent control) without physical contact. The apparatus consisted of three interconnected plexiglass chambers, each cylindrical in shape (15 cm long × 15 cm diameter) and arranged linearly. Mosquitoes were released into the central chamber, and each of the two outer chambers contained a smaller nylon-covered inner cylinder (10 cm long × 10 cm in diameter) that served as the odor source. Immediately before each test, 500 µL of DEET solution was applied to a nylon sock, allowed to air-dry for 5 minutes, and then fitted over the smaller inner cylinder before being placed into one of the designated outer chambers. Control odor sources were prepared identically using acetone alone. The DEET-treated and solvent-control odor cylinders were positioned symmetrically in the two outer chambers flanking the central release chamber.

For each assay, ten adult female mosquitoes of the specified strain were introduced into the central chamber via a small port in the middle of the central chamber, which had both ends sealed with plastic wrap, and acclimated for 20 minutes. The side chambers were connected to the central chamber, and the plastic wrap was gently removed from the connection part, exposing the mosquitoes to both odor chambers. To promote movement by positive phototaxis, the apparatus was surrounded with black cloth except for clear openings at both ends that allowed external light to enter. Mosquito movement was recorded for 8 minutes, after which the number of individuals in each chamber was counted. The apparatus was thoroughly washed with 70% ethanol and air-dried between replicates to eliminate residual volatiles. Each assay was repeated at least six times. The repellency index (RI) was calculated as: $RI = (Nc - Nt) / (Nc + Nt)$, where Nc is the number of mosquitoes in the control chamber and Nt is the number in the DEET-treated chamber.

Electroantennogram (EAG)

The electroantennogram (EAG) procedures were performed following the methods described by Chen et al[56]. The head of a female *Ae. aegypti* was excised and mounted onto an EAG holder equipped with two glass capillary electrodes. Each electrode was filled with 0.1% potassium chloride (KCl) and 0.5% polyvinylpyrrolidone (PVP), and chlorinated silver wires were inserted to establish electric contact. The excised head was positioned such that the base of the head connected to the reference electrode, while one antenna, with only an extremely small portion of the distal tip of the 13th antennal segment clipped to improve electrical continuity, was inserted into the recording electrode. The recording electrode was connected to a high-impedance AC/DC preamplifier (IDAC-2, Syntech, Germany).

During recording, the antenna was continuously exposed to a humidified airstream (20 ml/s). Odor stimuli pulses were delivered as 500-ms pulses injected into the airstream at the flow rate of 2 ml/s. DEET was formulated at the desired test concentration(s) using paraffin oil as the solvent. For each stimulus, 10 µL of the DEET solution was applied onto a 3 × 40 mm filter paper, inserted into a Pasteur pipette, and allowed to equilibrate for 30 seconds prior to use. Antennal responses were recorded for a total of 11 seconds, including a 1-second baseline period before the stimulus delivery. Consecutive stimuli were presented at a 30-second interval to minimize sensory adaptation.

Single sensillum recording (SSR)

Single sensillum recordings were performed as Liu et al with minor modifications[55]. An adult female *Ae. aegypti* (7-14 days old) was anesthetized on ice (~2 min) and immobilized inside a 200-µL pipette tip. The mosquito was then secured onto a block of dental wax using a coverslip mounted with double-sided tape. The tungsten reference electrode was inserted into the compound eye, and a tungsten recording electrode was advanced into an individual antennal sensillum under high magnification (x720) of a microscope (Leica Z6 Apo). Action potentials were preamplified using a Universal AC/DC Probe (10X Gain, Syntech) and digitized via an IDAC 4 interface (Syntech).

Test odorants were diluted to 1% (v/v) in paraffin oil. For each stimulus, 10 µL of odorant solution was applied to a 3 × 40 mm filter paper inserted into a glass Pasteur pipette to create a stimulus cartridge. After 30-s equilibration period, a 500-ms odor pulse was delivered using a Syntech CS-55 Stimulus Controller into a continuously humidified airstream airstream (20 mL/s) directed at the mosquito antenna. Action potential was recorded for a total of 11 seconds, including a 1-second per-stimulation baseline. Spike frequency was quantified as the differences in spike counts between 500 ms pre-stimulus period and 500 ms post-stimulus period, multiplied by 2 to convert to spikes/s.

The hierarchical cluster analysis of the response profile was conducted by PAST (4.17C) based on Euclidean distances and Complete linkage classification.

Fluorescence-guided SSR (FgSSR)

For fluorescence-guided single sensillum recording, a LED fluorescent illuminator (BGIMAGING BGI-P300-LG1.0) was used to visualize GFP-labeled sensilla prior to electrode insertion. After confirming fluorescence, electrophysiological recording proceeded identically to the conventional SSR protocol described above.

Two-electrode voltage clamp (TEVC)

cRNA was synthesized followed the procedure described in previous study with minor modifications[56]. Total RNA was isolated from approximately 500 *Ae. aegypti*

antennae using the acid guanidinium thiocyanate-phenol-chloroform method and treated with a TURBO DNase (Invitrogen) to remove genomic DNA. First-strand cDNA was synthesized from 1.5 µg of DNA-free RNA using SuperScript^{TM} IV with oligo(dT)$_{20}$ primers. Full-length coding sequences of target odorant receptors (Ors) were amplified by high-fidelity PCR (Q5 Polymerase, NEB) with gene-specific primers (Table S5), gel-purified, restriction-digested, and cloned into the pT7Ts vector. Plasmids were transformed into TOP10 *E. coli*, extracted, and sequencing verified by Sanger sequencing. The verified plasmids were linearized, and capped cRNA was generated using the mMESSAGE mMACHINE T7 Kit (Ambion) following the manufacturer's protocol.

TEVC recordings were performed as described[58]. Stage V-VI *Xenopus laevis* oocytes (Nasco, Salida, CA) were treated with collagenase I (GIBCO, Carlsbad, CA) in washing buffer (96 mM NaCl, 2 mM KCl, 5 mM $MgCl_2$•$6H_2O$, 5 mM HEPES sodium salt, and 10 µg/mL gentamycin, pH = 7.6) for ~1 hour at room temperature. Oocytes were then rinsed sequentially with 1× Ringer's solution, washing buffer, and modified Barth's saline (78 mM NaCl, 1 mM KCl, 0.33 mM $Ca(NO_3)_2$•$4H_2O$, 0.41 mM $CaCl_2$•$2H_2O$, 0.82 mM $MgSO_4$•$7H_2O$, 2.4 mM $NaHCO_3$, 10 µg/mL gentamycin, 10 µg/mL streptomycin, and 10 mM HEPES sodium salt, pH = 7.6) and incubated overnight at 18°C.

For expression of odorant receptors, each oocyte was injected with 20 nL of a premixed solution containing *AaegOr* and *AaegOrco* (both at 250 ng/µL) and incubated at 18°C for 4-7 days. Whole-cell odorant-evoked currents were recorded under voltage clamp (TEVC) (holding potential of -80 mV) using an OC-725C amplifier (Warner Instruments, Hamden, CT). Data were acquired and analyzed with Digidata 1440A and pCLAMP 10.2 (Axon Instruments Inc., CA). Odorants were initially dissolved in DMSO at 1:10 M and diluted to the desired concentrations (10^{-4} M) in ND96 solution (91 mM NaCl, 2 mM KCl, 1.8 mM $CaCl_2$•$2H_2O$, 2 mM $MgCl_2$•$6H_2O$, 5 mM HEPES sodium salt, pH = 7.6) immediately before application.

Ultra-low-input RNA sequencing of mosquito antennal flagellomeres

RNA-seq data for antennal flagellomeres of *Ae. aegypti* were generated using an optimized ultra-low-input RNA sequencing workflow. Adult mosquitoes were anesthetized on ice and proximal (flagellomeres 1-9) and distal (flagellomeres 10-13) antennal segments were microdissected into low-binding PCR tubes containing lysis buffer (Vazyme N712) supplemented with 0.2% Triton X-100 and 2 U/µL RNase-Inhibitor (Thermo Fisher Scientific). Three replicates were collected for each antennal region. Samples were immediately flash-frozen in liquid nitrogen to ensure rapid and complete lysis.

cDNA synthesis and whole transcriptome amplification were performed using the Vazyme WTA kit (N712). Amplified cDNA was purified with AMPure XP beads (Beckman Coulter, Cat. No. A63881) at a bead-to-sample ratio of 0.8:1, and assessed

using a Qubit 3.0 Fluorometer and Agilent Bioanalyzer 2100 to verify expected fragment sizes (~1000-2000 bp). Sequencing libraries were prepared using the TruePrep Flexible DNA Library Prep Kit for Illumina (Vazyme, TD504) and sequenced (paired-end 150 bp) on an Illumina NovaSeq X Plus platform. Raw reads were processed by adapter trimming and removal of low-quality reads. Clean reads were aligned to the *Ae. aegypti* genome (VectorBase) using Salmon, and transcript abundance was quantified as Transcripts Per Million (TPM).

CRISPR/CAS9 transgenesis

Single-guide RNAs (sgRNAs) were synthesized following previously described by Li [59] with minor modifications. sgRNAs targeting *AaegOr54* (AAEL015286) and *AaegOr55* (AAEL010415) were designed using the CHOPCHOP web tool (http://chopchop.cbu.uib.no/), scanning both sense and antisense strands for NGG protospacer-adjacent motifs (PAMs). Target sequences and primers were listed in Table S5. Linear double-stranded DNA (dsDNA) templates for each sgRNAs were generated by template-free PCR using Q5 High-Fidelity DNA Polymerase (NEB #M0491S). PCR amplification conditions were: 98 ºC for 30 s, followed by 35 cycles of 98 ºC for 10 s, 58 ºC for 10 s, and 72 ºC for 10 s, with a final extension at 72 ºC for 2 min. PCR products were purified using the Wizard SV Gel and PCR Clean-Up System (Promega #A9281). sgRNAs were transcribed using the MEGAscript T7 Kit (Ambion #AM1334), with 300 ng of purified DNA template per reaction. Resulting sgRNAs were purified using the MegaClear™ Kit (Ambion #AM1908), resuspended at 1000 ng/μL in nuclease-free water, and stored at −80 ºC in single-use aliquots. Recombinant Streptococcus pyogenes Cas9 protein (PNA Bio #CP01) was diluted to 1000 ng/μL, aliquoted, and stored at −80 ºC.

To generate the *AaegOr54*-QF2 driver line for the Q-system, *T2A-QF2-3xP3-DsRed* element was inserted into the *AaegOr54* coding region through CRISPR-mediated homologous recombination. The homologous template (donor plasmid) that contains *T2A-QF2-3xP3-DsRed* element, which was amplified from the *ppk301-T2A-QF2* HDR plasmid (Addgene plasmid# 130667)[33], flanked by ~1kb homologous arms was constructed using NEBuilder HiFi DNA Assembly kit (New England Biolabs). The left homologous arm was amplified with primer pair of HDR-*AaegOr54*LAF and HDR-*AaegOr54*LAR. The right homologous arm was amplified with primer pair of HDR-*AaegOr54*RAF and HDR-*AaegOr54*RAR . The primer pair for confirming the knock-in element was *AaegOr54*ExamF and *AaegOr54*ExamR. From the left homologous arm immediately preceding the *T2A*, 1 bp was removed to keep the *T2A* sequence in-frame. Red-eyed F1 mosquitoes were backcrossed for five generations and then crossed to the effector line to acquire progeny for *AaegOr54* localization studies. All primer sequences are listed in Table S5. Embryo collection and microinjection were performed according to Li et al[58] with minor adaptations. Adult females were blood fed five days prior to egg collection. A blackened oviposition cup lined with filter paper was placed in the cage under dark conditions. After 15-30 minutes, the cup was removed, and freshly laid (non-melanized) eggs were transferred

onto a glass slide and aligned on a moistened filter paper strip. Injection needles were pulled from the aluminosilicate capillaries using a Sutter P-1000 puller and beveled on a Sutter BV-10 microbeveler.

Microinjections were carried out under a compound microscope (100× magnification) using an Eppendorf FemtoJet injector. Approximately 50 embryos were injected per session. For generating the *AaegOr54*-QF2 driver line, the injection mixture contained Cas9 protein (300 ng/μL) premix with sgRNA (40 ng/μL) and donor plasmid (300 ng/μL). Injected embryos were transferred to water and maintained under standard rearing conditions until adulthood. The first generation (G0) of injected adults were separated based on sex and crossed to 5X wild-type counterparts. Their offspring (F1) were manually screened for DsRed-derived red eye fluorescence using an Compound Fluorescent Microscope (DP74, Olympus, Japan). Red-eyed F1 males were individually backcrossed to 5- fold females to establish a stable mutant line. DNA extraction was performed using FastPure Gel DNA Extraction (Vazyme Biotech, Nanjing) protocols and genomic DNA templates for PCR analyses of all individuals were performed (after mating) to validate the fluorescence marker insertion using primers that cover DSB sites. PCR products were sequenced to confirm the accuracy of the genomic insertion. Heterozygous mutant lines were thereafter backcrossed to wild-type *Ae. aegypti* for five generations before self-crossing and the progenies were used for screening homozygous individuals according to their DsRed-derived red eye fluorescence intensity. Putative homozygous mutant individuals were mated to each other and female adults laid eggs before being sacrificed for genomic DNA extraction and PCR analyses (as above) to confirm their homozygosity.
For generating the *AaegOr54*$^{-/-}$ and *AaegOr55*$^{-/-}$ *lines,* the injection mixture contained Cas9 protein (300 ng/μL) premix with sgRNA (40 ng/μL). Injected embryos were transferred to water and maintained under standard rearing conditions until adulthood. The first generation (G0) of injected adults were separated based on sex and crossed to 5X wild-type counterparts. Their offspring (F1) were screened by clipping one hind leg from each adult for genomic DNA extraction using the DNeasy Blood & Tissue Kit (QIAGEN) and PCR amplification of the target locus was performed using *AaegOr54*- or *AaegOr55*-specific primers, *AaegOr54*ExamF/*AaegOr54*ExamR and *AaegOr55*ExamF/*AaegOr55*ExamR, respectively (Table S5). PCR amplicons were Sanger-sequenced to identify indel mutations. Detailed sequencing results of the mutant mosquitoes are provided in Table S4.

Drosophila empty neuron expression system

To generate the *UAS-AaegOr54* construct for transgenic *Drosophila melanogaster*, we employed a seamless homologous recombination strategy[32]. Total RNA was extracted from approximately 100 dissected *Ae. aegypti* antennae preserved in Trizol (Invitrogen, Carlsbad, CA, USA). The full-length coding sequence of *AaegOr54* was amplified with primers (Table S5) according to flanking homology arms designed from VectorBase reference sequence (https://www.vectorbase.org). The pUASTattB vector (Addgene #96148) was linearized by PCR using Phusion High-Fidelity DNA

Polymerase (New England Biolabs, Ipswich, MA, USA) and primers listed in Table S5. The *AaegOr54* insert was assembled into the vector using the pEASY-Basic Seamless Cloning and Assembly Kit (TransGen Biotech, Beijing, China). Recombinant constructs were transformed into Trans1-T1 Phage Resistant Chemically Competent Cells (TransGen Biotech) and positive clones were verified and purified using the Plasmid Mini Kit (Omega Bio-Tek, Norcross, GA, USA) prior to microinjection.

Heterologous expression of *AaegOr54* in the *Drosophila* ab3A "empty neuron" system followed two-stage genetic crossing as described by Chahda et al [32]. The *UAS-AaegOr54* plasmid was microinjected into a *Drosophila* strain containing a white-eye rescue marker, generating transgenic flies with red eyes (genotype: w; +; *UAS-AaegOr54*(w+)/+). The ab3A empty neuron driving line (*Or22ab*$^{-/-}$*-Gal4/Cyo*) and the balancer line (*sp/Cyo; Dr/Tm3*) were gifts from Dr. John Carlson (Yale University).

To generate the expression line, we first generated an intermediate genotype (*Or22ab*$^{-/-}$*-Gal4*/*Cyo*; *Dr*/*Tm3*), identified by curly wings and stubble bristles, and then self-crossed it to obtain a homozygous empty neuron line (*Or22ab*$^{-/-}$*-Gal4/Or22ab*$^{-/-}$*-Gal4; Dr/Tm3*) with straight wings and stubble bristles. In parallel, the *UAS-AaegOr54* insertion line was balanced to produce *Sp/Cyo; UAS-AaegOr54/Tm3*. Crossing the homozygous empty neuron driver to the balanced *UAS-AaegOr54 line* produced progeny of genotype *Or22ab*$^{-/-}$*-Gal4/Cyo; UAS-AaegOr54/Tm3*, recognized by orange eyes, curly wings, and stubble bristles. Self-crossed these flies yielded the stable homozygous expression line (*Or22ab*$^{-/-}$*-Gal4/Or22ab*$^{-/-}$*-Gal4; UAS-AaegOr54/UAS-AaegOr54*), which expresses the mosquito receptor exclusively in the ab3A empty neuron. Adult flies of this final genotype were used for single sensillum recordings.

Brain immunofluorescence

Brain dissection and immunofluorescence staining were performed as previously described[33] with minor modification. Adult female mosquitoes (6- to 14-day-old) were anesthetized on ice, and heads were removed by gently pinching the cervix with fine forceps. Excised heads were fixed in phosphate-buffered saline (PBS) containing 4% paraformaldehyde, and 0.25% Triton X-100 for 3 hours on a nutator. Brains were then dissected from the head capsules in ice-cold PBS and transferred to a 48-well plate.

All subsequent steps were conducted with gentle agitation on a low-speed orbital shaker. Brains were washed six times for 15 minutes each in PBS containing 0.25% Triton X-100 (PBT) at room temperature, followed by permeabilization ~48 hours at 4 ºC in PBS supplemented with 4% Triton X-100 and 2% normal goat serum (NGS). After permeabilization, brains were washed again six times in PBT and incubated for ~48 hours at 4 ºC with primary antibodies diluted in PBT containing 2% NGS. The primary antibodies included mouse anti-dmBrp (NC82, DSHB; 1:50) to label synaptic

neuropil, and rabbit anti-GFP (A11122, Life Technologies; 1:10,000).

Following primary antibody incubation, brains were washed six times in PBT and then incubated for an additional ~48 hours at 4 ºC with secondary antibodies - goat anti-mouse Cy5 (115-605-003, Jackson ImmunoResearch; 1:250) and goat anti-rabbit-Alexa Fluor 488 (111-545-003, Jackson ImmunoResearch; 1:500) - diluted in PBT with 2% NGS. Afterward, brains received a final series of six 15-minute washes in PBT. Prior to imaging, brains were equilibrated overnight in mounting medium (P0126, Beyotime) and subsequently mounted in the same medium.

Female antennal lobe confocal imaging

Confocal imaging of mosquito brains was performed using an Andor Dragonfly confocal microscope system (CR-DFLY-202-2540) equipped with a 20X objective. Antennal lobes were acquired at resolutions of 1024 × 1024 pixels in the xy-plane with a z-step size of 1 µm. Laser power and detector gain were incrementally adjusted along the z-axis to compensate for signal attenuation with imaging depth. Care was taken to avoid signal saturation while ensuring sufficient contrast to visualize the deepest glomeruli for subsequent segmentation. All imaging acquisition was optimized for reliable visualization of glomerular boundaries and for determining the presence or absence of specific fluorescence labeling, rather than for quantitative intensity measurements.

To distinguish specific neuronal expression patterns, we used the 3xP3 promoter-driven fluorescent reporters in both knock-in and QUAS transgenic lines. The 3xP3 promoter drives expression primarily in the optic lobes and in a subset of dorsal brain neurons, regions that do not overlap with the antennal lobe. Consistent with prior reports (*33*), no 3xP3-derived fluorescence was detected in the antennal lobes of reporter-only controls (data not shown). For clarity in the representative figures, representative images of antennal lobes were cropped to remove 3xP3-derived fluorescence signal originating in other brain regions.

Antennal lobe 3D reconstruction

Three-dimensional reconstruction and glomerular segmentation were performed using Imaris 10.1.0 (Bitplane, UK). Confocal image stacks were imported into Imaris, and each glomerulus was manually delineated by tracing its boundary in every optical section based on immunohistochemical staining. Surface rendered 3D models were generated from these segmented contours. Glomeruli were identified and named following the neuroaxis-based nomenclature[27, 35], using two-letter codes denoting relative positions: anterior (A), posterior (P), ventral (V), dorsal (D), lateral (L), medial (M).

Data analysis and statistics

All statistical analyses were performed using Prism 10 (GraphPad Software). Data are presented as mean ± s.e.m. Statistical significance was defined as $P < 0.05$. The

879 specific statistical tests, sample sizes, and replication details used for each experiment
880 are provided in figure legends.
881
882 **References**
883 1. Leal, W. S. Odorant reception in insects: roles of receptors, binding proteins, and
884 degrading enzymes. *Annu. Rev. Entomol.*, **58**, 373-391 (2013).
885 2. Herre, M. *et al.* Non-canonical odor coding in the mosquito. *Cell* **185**, 3104-
886 3123.e28 (2022).
887 3. Matthews, B. J., McBride, C. S., DeGennaro, M., Despo, O. & Vosshall, L. B. The
888 neurotranscriptome of the *Aedes aegypti* mosquito. *BMC Genomics* **17**, 32 (2016).
889 4. Raji, J. I. & Potter, C. J. Chemosensory ionotropic receptors in human host-seeking
890 mosquitoes. *Curr. Opin. Insect. Sci.* **54**, 100967 (2022).
891 5. Wolff, G. H. & Riffell, J. A. Olfaction, experience and neural mechanisms
892 underlying mosquito host preference. *J. Exp. Biol.* **221**, (2018).
893 6. Wang, Y. *et al.* Structural basis for odorant recognition of the insect odorant
894 receptor OR-Orco heterocomplex. *Science* **384**, 1453–1460 (2024).
895 7. Zhao, J., Chen, A. Q., Ryu, J. & Del Mármol, J. Structural basis of odor sensing by
896 insect heteromeric odorant receptors. *Science* **384**, 6703 (2024)
897 8. McCabe, E. T., Barthel, W. F., Gertler, S. I. & Hall, S. A. Insect repellents. III. N,N-
898 diethylamides1. *ACS Publications* .
899 9. Debboun, M., Frances, S. P., Strickman D. *Insect repellents: principles, methods,*
900 *and uses*. (CRC Press, Boca Raton, 2006).
901 10. Rutledge, L. C., Wirtz, R. A., Buescher, M. D. & Mehr, Z. A. Mathematical
902 models of the effectiveness and persistence of mosquito repellents. *J. Am. Mosq.*
903 *Control. Assoc.* **1**, 56–62 (1985).
904 11. Schofield, S. & Plourde, P. Statement on personal protective measures to prevent
905 arthropod bites. *Can. Commun. Dis. Rep.* **38**, 1–18 (2012).
906 12. Briassoulis, G., Narlioglou, M. & Hatzis, T. Toxic encephalopathy associated
907 with use of DEET insect repellents: a case analysis of its toxicity in children. *Hum.*
908 *Exp. Toxicol.* **20**, 8–14 (2001).
909 13. Osimitz, T. G. & Murphy, J. V. Neurological effects associated with use of the
910 insect repellent N, N-Diethyl-m-toluamide (DEET). *J. Toxicol. Clin.* **35**, 435–441
911 (1997).
912 14. Snyder, J. W., Poe, R. O., Stubbins, J. F. & Garrettson, L. K. Acute manic
913 psychosis following the dermal application of N,N-diethyl-m-toluamide (deet) in an
914 adult. *J. Toxicol. Clin.* **24**, 429–439 (1986).
915 15. Fradin, M. S. & Day, J. F. Comparative efficacy of insect repellents against
916 mosquito bites. *New Engl. J. Med.* **347**, 13–18 (2002).
917 16. Wylie, B. J., Hauptman, M., Woolf, A. D. & Goldman, R. H. Insect repellants
918 during pregnancy in the era of the Zika virus. *Obstetrics & Gynecology* **128**, 1111
919 (2016).
920 17. Fatou, M. & Müller, P. In the arm-in-cage test, topical repellents activate
921 mosquitoes to disengage upon contact instead of repelling them at distance. *Sci.*
922 *Rep.* **14**, 24745 (2024).

18. Brown, M. & Hebert, A. A. Insect repellents: an overview. *J. Am. Acad. Dermatol.* **36**, 243–249 (1997).
19. DeGennaro, M. The mysterious multi-modal repellency of DEET. *Fly* **9**, 45–51 (2015).
20. Koren, G., Matsui, D. & Bailey, B. DEET-based insect repellents: safety implications for children and pregnant and lactating women.*Can. Med. Assoc. J.* **169**, 209–212 (2003).
21. Afify, A., Betz, J. F., Riabinina, O., Lahondère, C. & Potter, C. J. Commonly Used Insect Repellents Hide Human Odors from *Anopheles* Mosquitoes. *Curr. Biol.* **29**, 3669-3680.e5 (2019).
22. DeGennaro, M. *et al.* orco mutant mosquitoes lose strong preference for humans and are not repelled by volatile DEET. *Nature* **498**, 487–491 (2013).
23. Valbon, W. *et al.* Bioallethrin activates specific olfactory sensory neurons and elicits spatial repellency in *Aedes aegypti*. *Pest Manag. Sci.* **78**, 438–445 (2022).
24. Xu, P., Choo, Y.-M., Rosa, A. D. L. & Leal, W. S. Mosquito odorant receptor for DEET and methyl jasmonate. *Proc. Natl. Acad. Sci. U.S.A.* **111**, 16592–16597 (2014).
25. Powell, J. R., Gloria-Soria, A. & Kotsakiozi, P. Recent history of *Aedes aegypti*: vector genomics and epidemiology records. *BioScience* **68**, 854–860 (2018).
26. Fernandez Triana, M. *et al.* Grapefruit-derived nootkatone potentiates GABAergic signaling and acts as a dual-action mosquito repellent and insecticide. *Curr. Biol.* **35**, 177-186 (2024).
27. Ghaninia, M., Ignell, R. & Hansson, B. S. Functional classification and central nervous projections of olfactory receptor neurons housed in antennal trichoid sensilla of female yellow fever mosquitoes, *Aedes aegypti*. *Eur. J. Neurosci.* **26**, 1611–1623 (2007).
28. Syed, Z. & Leal, W. S. Mosquitoes smell and avoid the insect repellent DEET. *Proc. Natl. Acad. Sci. U.S.A.* **105**, 13598–13603 (2008).
29. Liu, F., Chen, L., Appel, A. G. & Liu, N. Olfactory responses of the antennal trichoid sensilla to chemical repellents in the mosquito, *Culex quinquefasciatu*s. *J. Insect Physiol.* **59**, 1169–1177 (2013).
30. Stanczyk, N. M., Brookfield, J. F. Y., Ignell, R., Logan, J. G. & Field, L. M. Behavioral insensitivity to DEET in *Aedes aegypti* is a genetically determined trait residing in changes in sensillum function. *Proc. Natl. Acad. Sci. U.S.A.* **107**, 8575–8580 (2010).
31. Ditzen, M., Pellegrino, M. & Vosshall, L. B. Insect odorant receptors are molecular targets of the insect repellent DEET. *Science* **319**, 1838–1842 (2008).
32. Chahda, J. S., Soni, N., Sun, J. S., Ebrahim, S. A., Weiss, B. L., & Carlson, J. R. . The molecular and cellular basis of olfactory response to tsetse fly attractants. PLoS genetics, **15(3)**, e1008005 (2019).
33. Riabinina, O., Task, D., Marr, E. et al. Organization of olfactory centres in the malaria mosquito *Anopheles gambiae*. *Nat Commun* **7**, 13010 (2016).
34. Ignell, R., Dekker, T., Ghaninia, M. & Hansson, B. S. Neuronal architecture of the mosquito deutocerebrum. *J. Comp. Neurol.* **493**, 207–240 (2005).

35. Shankar, S. & McMeniman, C. J. An updated antennal lobe atlas for the yellow fever mosquito *Aedes aegypti*. *PLoS Negl. Trop. Dis.* **14**, e0008729 (2020).
36. Bohbot, J. D. & Dickens, J. C. Insect repellents: modulators of mosquito odorant receptor activity. *PLoS One* **5**, e12138 (2010).
37. Pellegrino, M., Steinbach, N., Stensmyr, M. C., Hansson, B. S. & Vosshall, L. B. A natural polymorphism alters odour and DEET sensitivity in an insect odorant receptor. *Nature* **478**, 511–514 (2011).
38. Wang, X., Chen, Z. & Liu, N. Dual mechanisms of synthetic repellents in *Aedes aegypti*: odorant receptor inhibition and odor volatility modulation. *Entomol. Gen.* **45**, 1475–1487 (2025).
39. Liu, F., Xia, X. & Liu, N. Molecular basis of N,N-diethyl-3-methylbenzamide (DEET) in repelling the common bed bug, *Cimex lectularius*. *Front. Physiol.* **8**, (2017).
40. Goldman, O. V., DeFoe, A. E., Qi, Y., Jiao, Y., Weng, S. C., Wick, B., ... & Shai, N. A single-nucleus transcriptomic atlas of the adult *Aedes aegypti* mosquito. *Cell*, **188(25)**, 7267-7290 (2025).
41. Adavi, E. D., Anjos, V. L., Kotb, S., Metz, H. C., Tian, D., Zhao, Z., ... & McBride, C. S. Olfactory receptor coexpression and co-option in the dengue mosquito. *Biorxiv*. (2024).
42. Barbieri, F. *et al.* Mediterranean plants and spices as a source of bioactive essential oils for food applications: chemical characterisation and in vitro activity. *Int. J. Mol. Sci.* **26**, 3875 (2025).
43. Moullamri, M. *et al. Salvia officinalis*, *Lavandula angustifolia*, and *Mentha pulegium* essential oils: insecticidal activities and feeding deterrence against *Plodia interpunctella* (Lepidoptera: Pyralidae). *J. Essent. Oil-Bear. Plants.* **27**, 16–33 (2024).
44. Norris, E. J., Kline, J. & Bloomquist, J. R. Repellency and toxicity of vapor-active benzaldehydes against *Aedes aegypti*. *ACS Infect. Dis.* **10**, 120–126 (2024).
45. Smallegange, R. C. *et al.* Malaria infected mosquitoes express enhanced attraction to human odor. *PLoS One* **8**, e63602 (2013).
46. Mostafiz, M. M., Jhan, P. K., Shim, J.-K. & Lee, K.-Y. Methyl benzoate exhibits insecticidal and repellent activities against *Bemisia tabaci* (Gennadius) (Hemiptera: Aleyrodidae). *PLOS ONE* **13**, e0208552 (2018).
47. Strickland, J., Larson, N. R., Feldlaufer, M. & Zhang, A. Characterizing repellencies of methyl benzoate and its analogs against the common bed bug, *Cimex lectularius*. *Insects* **13**, 1060 (2022).
48. Singh, P. *et al.* Combinatorial encoding of odors in the mosquito antennal lobe. *Nat Commun* **14**, 3539 (2023).
49. Lahondere, C., Vinauger, C., Okubo, R. P., Wolff, G. H., Chan, J. K., Akbari, O. S., & Riffell, J. A. . The olfactory basis of orchid pollination by mosquitoes. *Proc. Natl. Acad. Sci. U.S.A.* **117**, 708-716 (2020).
50. Raji, J. I., Konopka, J. K. & Potter, C. J. A spatial map of antennal-expressed ionotropic receptors in the malaria mosquito. *Cell Rep.* **42**, 112101 (2023).

51. Wang, G., Carey, A. F., Carlson, J. R. & Zwiebel, L. J. Molecular basis of odor coding in the malaria vector mosquito *Anopheles gambiae*. *Proc. Natl. Acad. Sci. U.S.A.* **107**, 4418–4423 (2010).
52. Carey, A. F., Wang, G., Su, C.-Y., Zwiebel, L. J.& Carlson, J. R. Odorant reception in the malaria mosquito *Anopheles gambiae*. *Nature* **464**, 66-71 (2010)
53. Dennis, E. J., Goldman, O. V. & Vosshall, L. B. *Aedes aegypti* mosquitoes use their legs to sense DEET on contact. *Curr. Biol.* **29**, 1551-1556.e5 (2019).
54. Lee, Y., Kim, S. H. & Montell, C. Avoiding DEET through insect gustatory receptors. *Neuron* **67**, 555–561 (2010).
55. Liu, F., Wang, Q., Xu, P., Andreazza, F., Valbon, W. R., Bandason, E., Chen, M., Yan, R., Feng, B., B. L., Smith, Scott, J. G., Takamatsu, G., Ihara, M., Matsuda, K., Klimavicz, J., Coats, J., Oliveira, E. E., Du, Y., Dong, K. A dual-target molecular mechanism of pyrethrum repellency against mosquitoes. *Nat*. Commun. **12**, 2553 (2021).
56. Chen, Z., Wang, X., Liu, F., Jia, X., Liu, N. Chemical antagonistic effects on the human odor-evoked responses of yellow fever mosquito, *Aedes aegypti*. *Entomol. Gen.* **43,** 4 (2023).
57. Liu, F., Liu, N. Using Single sensillum recording to detect olfactory neuron responses of bed bugs to semiochemicals. *J. Vis. Exp.*,**107**, 53337 (2016).
58. Wang, X., Heterologous expression and functional analysis of *Aedes aegypti* odorant receptors to human odors in *Xenopus* oocytes. *J. Vis. Exp.*,**172**, e61813 (2021).
59. Li, M., Bui, M., Yang, T., Bowman, C. S., White, B. J., Akbari, O. S. Germline Cas9 expression yields highly efficient genome engineering in a major worldwide disease vector, *Aedes aegypti*. *Proc. Natl. Acad. Sci. U.S.A.* **114**, e10540–e10549 (2017).

Acknowledgements: We thank Dr. Leslie Vosshall and her group for providing the QUAS-mCD8:GFP reporter strain. We thank Dr. John Carlson for providing the Gal4 line (*w; Cyo/Δhalo; Or22a-Gal4*). We also acknowledge the Biosafety Level 2 (BSL-2) and Animal Biosafety Level 2 (ABSL-2) Laboratories at the Institute of Infectious Diseases, Shenzhen Bay Laboratory, for their support and assistance in this research.

Author contributions: N.L., F.L., Z.C., X.W., and W.S.L. conceptualized the project. X.W., Q.Q., and Y.W. conducted SSR and EAG experiments. R.Y. and M.C. performed FgSSR. D.J.B., X.W., and Y.W. generated the *AaegOr54*-QF2 lines. X.F. and D.J.B. generated the *AaegOr55* knockout lines. X.W. and D.J.B. performed hand-in-cage and uniport olfactometer assay experiments. X.W., R.Y, Z.C., S.L., and Y.W. performed plasmid construction and TEVC experiments. Y.W. and Q.Q. performed ultra-low-input RNA sequencing and analysis. X.W. and H.Z. performed brain immunofluorescence and antennal lobe 3D reconstruction. N.L., F.L., X.W., and W.S.L. wrote and edited the manuscript. All authors read and approved the manuscript.

Competing interest: The authors declare no competing or financial interests.

Data, code, and materials availability: All relevant data are within the manuscript and its supporting information files.

Funding: The project described was supported by Award Number R03AI159700 to N.L. from the National Institute of Allergy and Infectious Diseases (NIH), AAES Hatch/Multistate Grants ALA015-1-16009, ALA015-1-19148 to NL, National Natural Science Foundation of China Grants 82372289 to F.L., and the China Postdoctoral Science Foundation (2024M752152) to Q.Q. Research conducted at the University of California, Davis, was supported by gifts from various donors to the university.

Extended Data for

DEET Olfactory Reception in the Yellow Fever Mosquito

Xin Wang[1,2]†, Ru Yan[3]†, Dylan J. Brown[1]†, Qian Qi[2]†, Xuechun Feng[1,4], Zhou Chen[1], Yanjie Wang[5], Yifan Wang[1], Simin Liang[2], Heng Zhang[2], Mengli Chen[6], Yinliang Wang[7], Walter S. Leal[8*], Feng Liu[2,9*], and Nannan Liu[1*]

Affiliations:

[1]Department of Entomology and Plant Pathology, Auburn University, Auburn, USA
[2]Institute of Infectious Diseases, Shenzhen Bay Laboratory, Shenzhen, China
[3]College of Life Sciences, Zhejiang Chinese Medical University, Hangzhou
[4]School of Agriculture and Biotechnology, Zhejiang University, Hangzhou, China
[5]Genomics core, Biomedical Research Core Facilities, Shenzhen Bay Laboratory, Shenzhen, China
[6]College of Advanced Agricultural Sciences, Zhejiang A&F University, Hangzhou, China
[7]Agriculture Gene Engineering Research Center of the Ministry of Education, Northeast Normal University, Changchun 130024, China
[8]Department of Molecular and Cellular Biology, University of California-Davis, Davis, CA, USA
[9]Guangdong Provincial Key Laboratory of Infection Immunity and Inflammation, Shenzhen, China

†These authors contributed equally to this work
*Co-corresponding authors. Email: N.L. (liunann@auburn.edu); F.L. (liufeng@szbl.ac.cn), W.S.L (wsleal@ucdavis.edu)

This PDF file includes:

Figs S1 to S7
Tables S1 to S5

Extended Data

Figs. S1 to S6

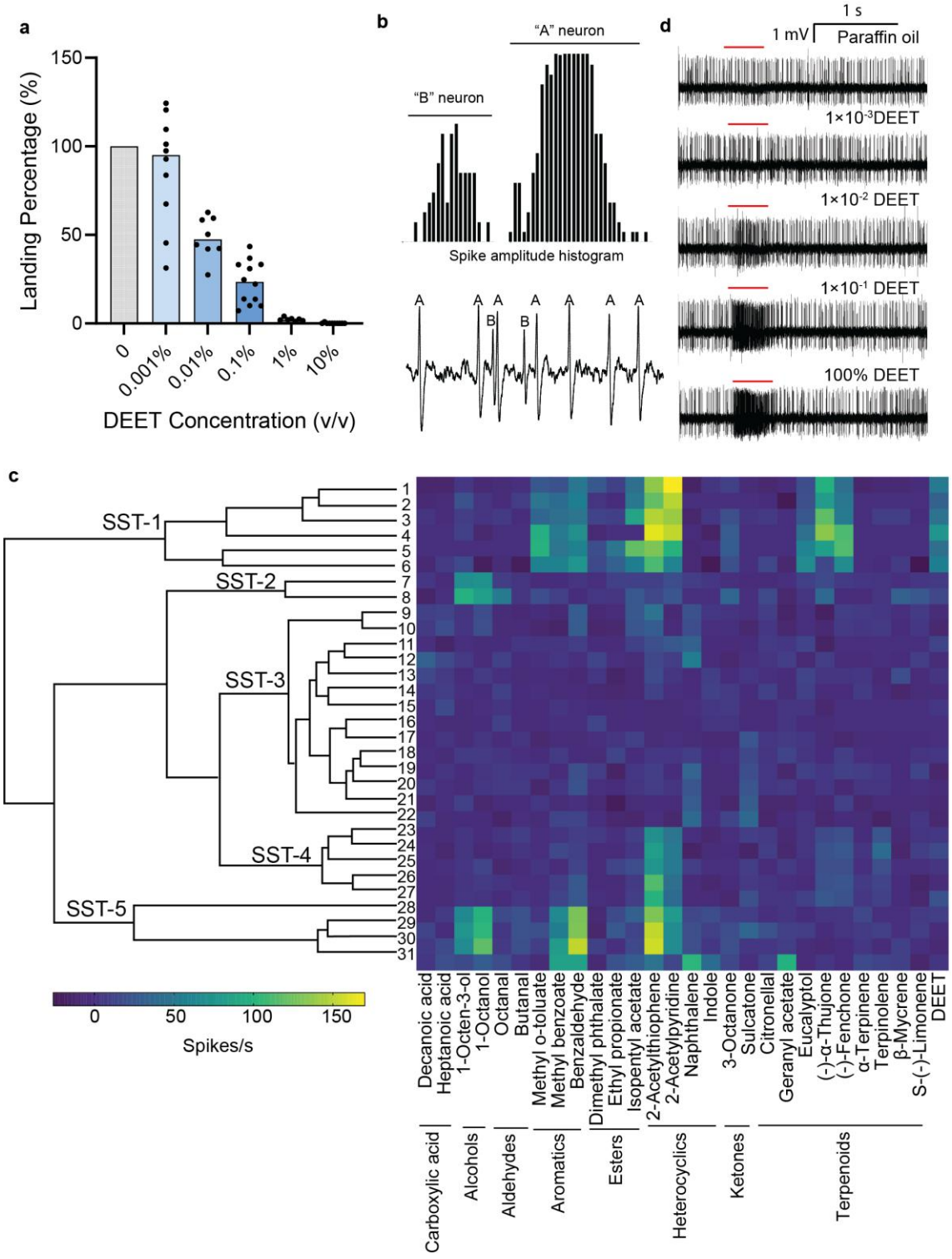

Fig. S1. Behavioral and electrophysiological responses of *Ae. aegypti* to DEET. a, Effect of DEET concentration on landing percentage in WT *Ae. aegypti* females. **b,** Distinct spontaneous neuronal activities were distinguishable based on spike amplitude, with larger amplitudes corresponding to "A" neurons and the smaller

amplitudes to “B” neurons (top). The distribution of spike amplitudes is also shown (bottom). **c,** Dendrogram from complete linkage cluster analysis of 31 ORNs housed in SST sensilla, based on their response profiles to 28 tested compounds. Five major clusters Were identified. **d,** Representative SSR traces from WT mosquitoes exposed to increasing concentrations of DEET (1×10^{-3} v/v to 100%; paraffin oil served as solvent).

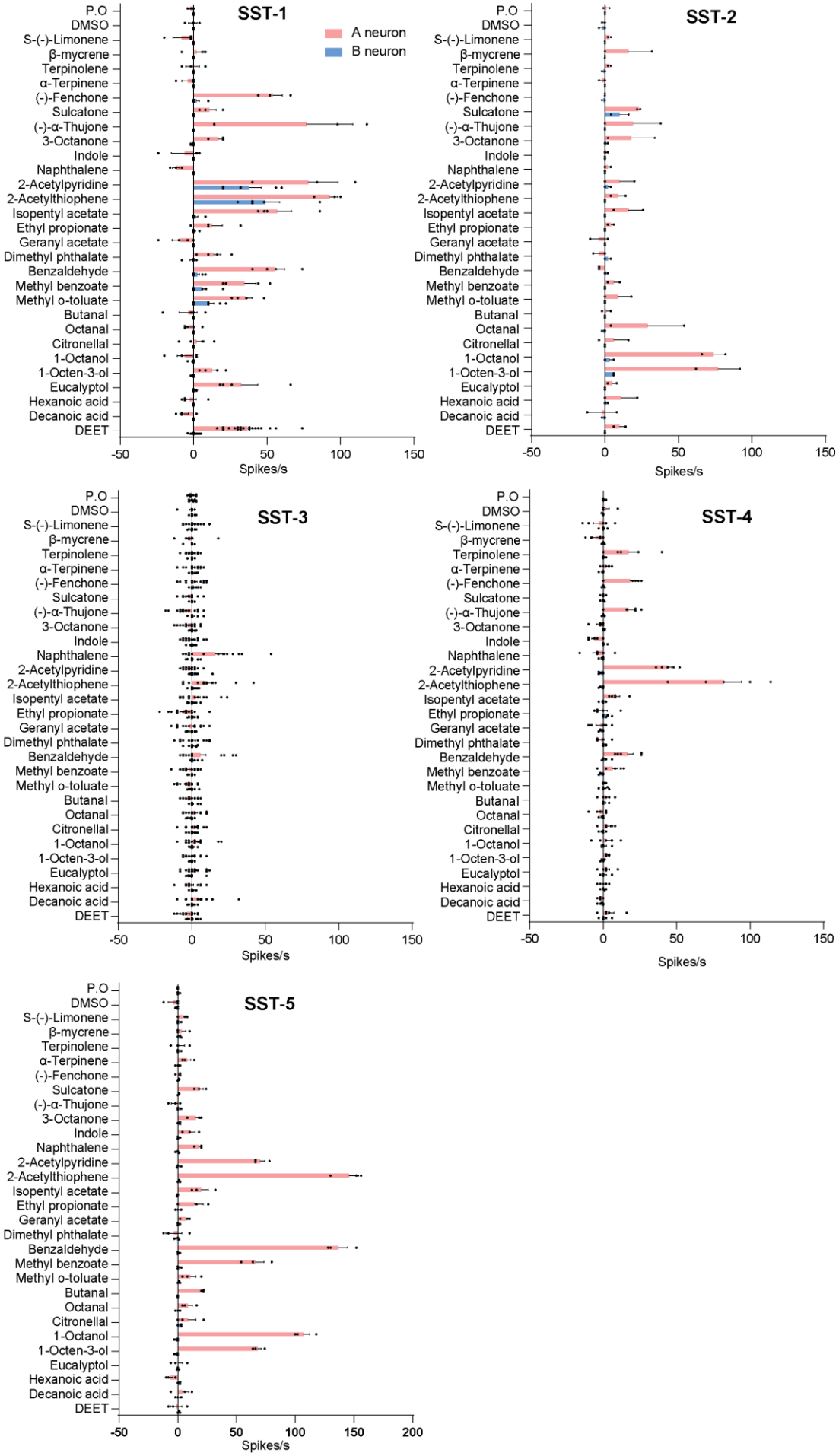

Fig. S2. Response profiles of SST sensilla identified by the single sensillum recording. Data are presented as mean ± s.e.m., with individual data points shown for each biological replicate. Solvents used were paraffin oil (P.O) or DMSO.

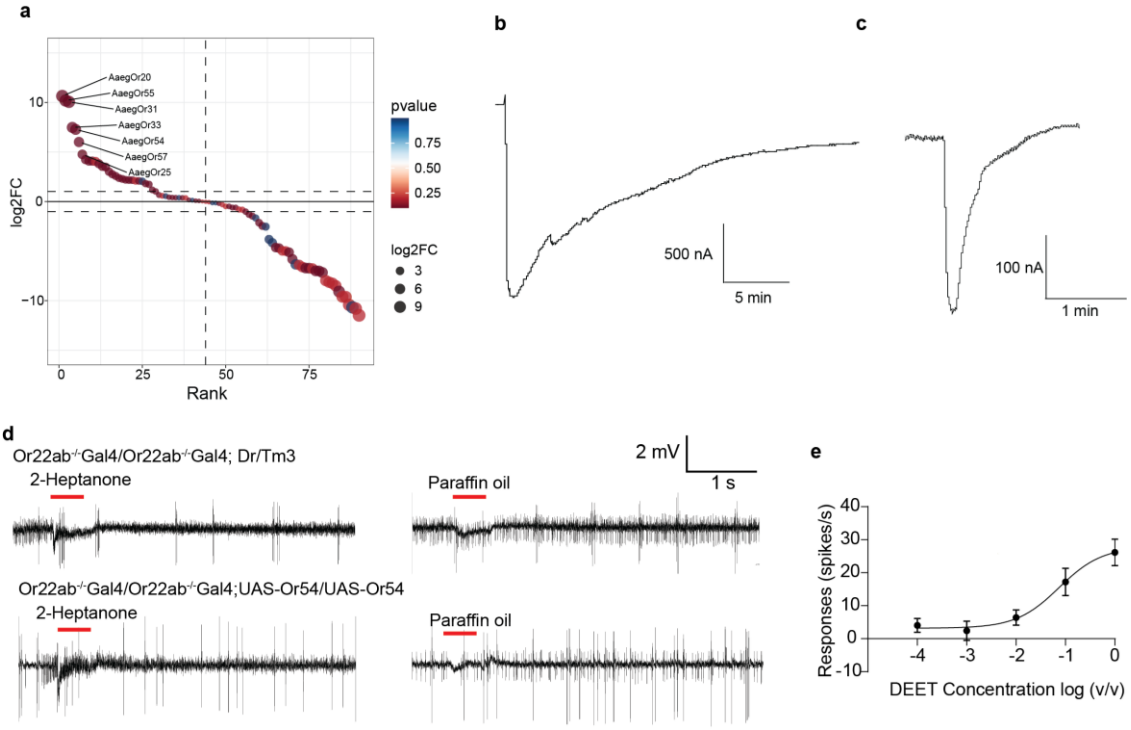

Fig. S3. Identification of *AaegOr54* in *Ae. Aegypti*. a, Comparison of odorant receptor gene expression between the proximal antennal region (flagellomeres 1-9) and the distal region (flagellomeres 10-13). Genes are ordered from left to right according to decreasing fold-enrichment in the distal region. The y-axis shows fold-change values on a $\log_2$ scale. **b,** Representative two-electrode voltage-clamp (TEVC) traces showing *AaegOr54* responses to DEET (10^{-4} M). **c,** Representative TEVC traces showing *AaegOr55* responses to DEET (10^{-4} M). **d,** Representative SSR traces from control fruit flies (*Or22*ab$^{-/-}$; *Dr*/*TM3*, top) and transgenic flies expressing *AaegOr54* (*Or22*ab$^{-/-}$; *UAS-AaegOr54*, bottom) in the ab3A neuron in response to 2-heptanone and paraffin oil (solvent). **e,** Dose-dependent SSR responses to DEET in transgenic lines expressing *AaegOr54* in *Drosophila* expression system (n = 5-8).

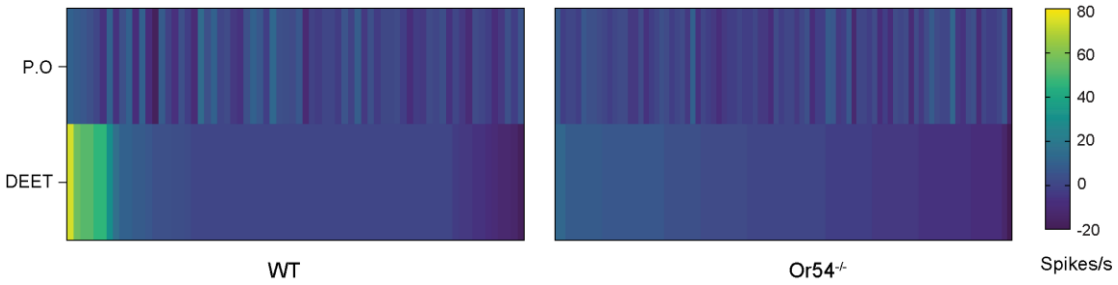

Fig. S4. Comparison of SSR recordings before and after OR54 knockout. Heatmaps depicting neuronal responses from SSR recordings to paraffin oil (P.O.) and DEET (10^{-2} v/v) in WT (70 records) and *AaegOr54*$^{-/-}$ (88 records) strains. Response

amplitudes range from -20 spikes/s (dark blue) to 80 spikes/s (yellow). Each column indicates the SSR recording from different individual sensillum, P.O served as a negative control.

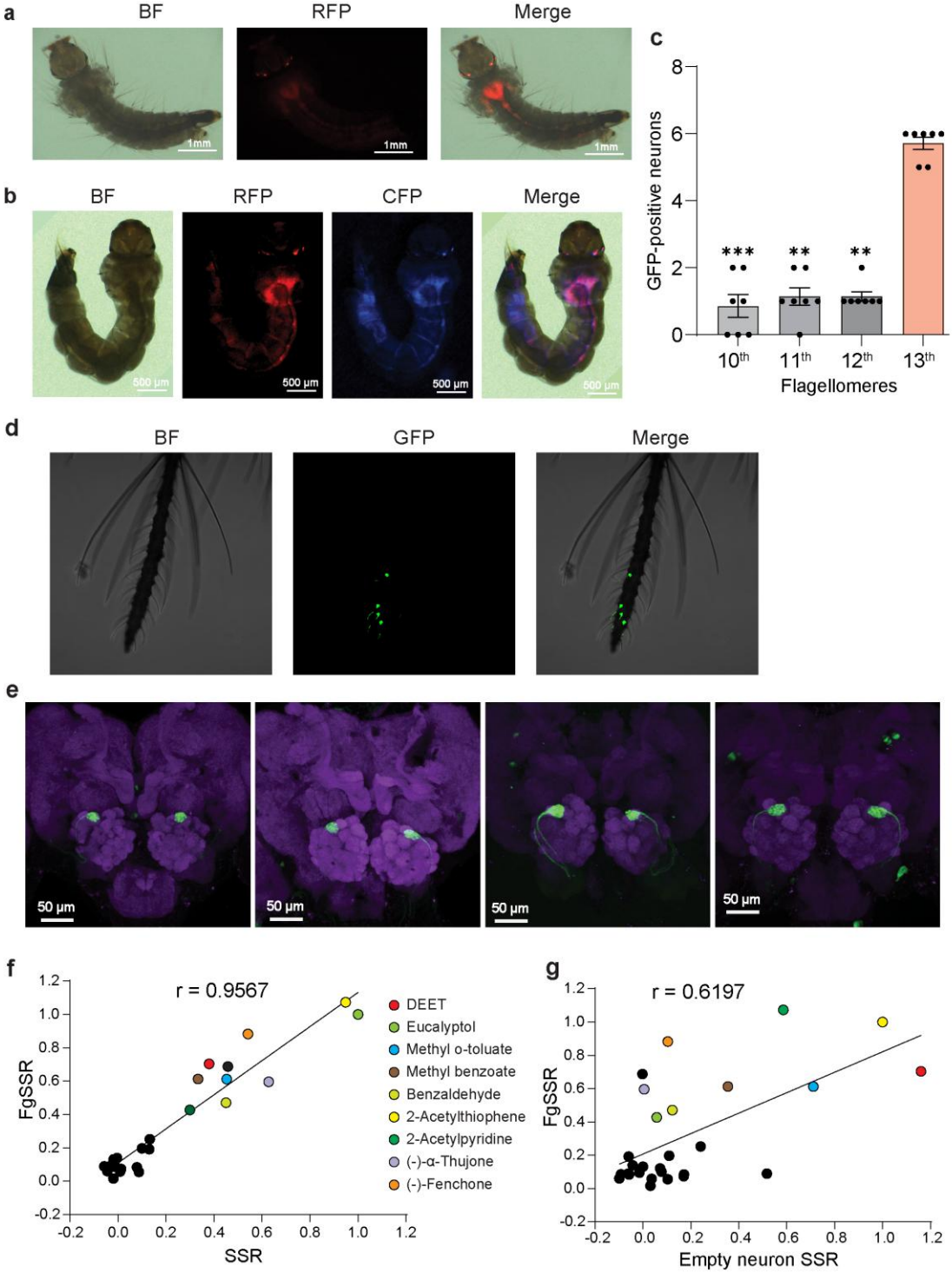

Fig. S5. Fluorescent labeling of *AaegOr54*-QF2 transgenic mosquitoes. a, Representative images of the *AaegOr54*-QF2 knock-in line showing DsRed fluorescence driven by the *3×P3* promoter in larval eyes. **b,** Representative images of *AaegOr54*$^{+/QF2}$ > *QUAS-mCD8:GFP* larvae showing both DsRed (*3×P3-DsRed*) and

CFP (*3×P3-CFP*) fluorescence in the eyes. **c,** Bar chart summarizing the average number of *AaegOR54*-positive cell populations across the 10^{th}-13^{th} antenna flagellomeres (n=7). Statistical analysis was performed using a Kruskal–Wallis test followed by Dunn's multiple-comparisons test (**$0.001 < P < 0.01$; ***$0.0001 < P < 0.001$). **d,** Representative maximum-intensity projections of confocal z-stacks showing GFP-labeled SST sensilla on the 13th flagellomere of male antenna. **e,** Maximum-intensity projections of four additional adult female brains showing GFP-labeled axons of *AaegOr54*-expressing neurons innervating the antennal lobe. **f,** Correlation analysis of SST-1 response profiles obtained from wild-type SSR and fluorescence-guided SSR (FgSSR). Responses were normalized to 2-acetylthiophene (set to 1), which elicited the strongest response. Compounds eliciting strong response were labelled with different colors while other compounds eliciting weak response were labelled as black dots. **g.** Correlation analysis of response profiles obtained by FgSSR and the the *Drosophila* epmty neuron expression system. Responses were normalized to 2-acetylthiophene (set to 1), which elicited the strongest response. Compounds eliciting strong response were labelled with different colors while other compounds eliciting weak response were labelled as black dots.

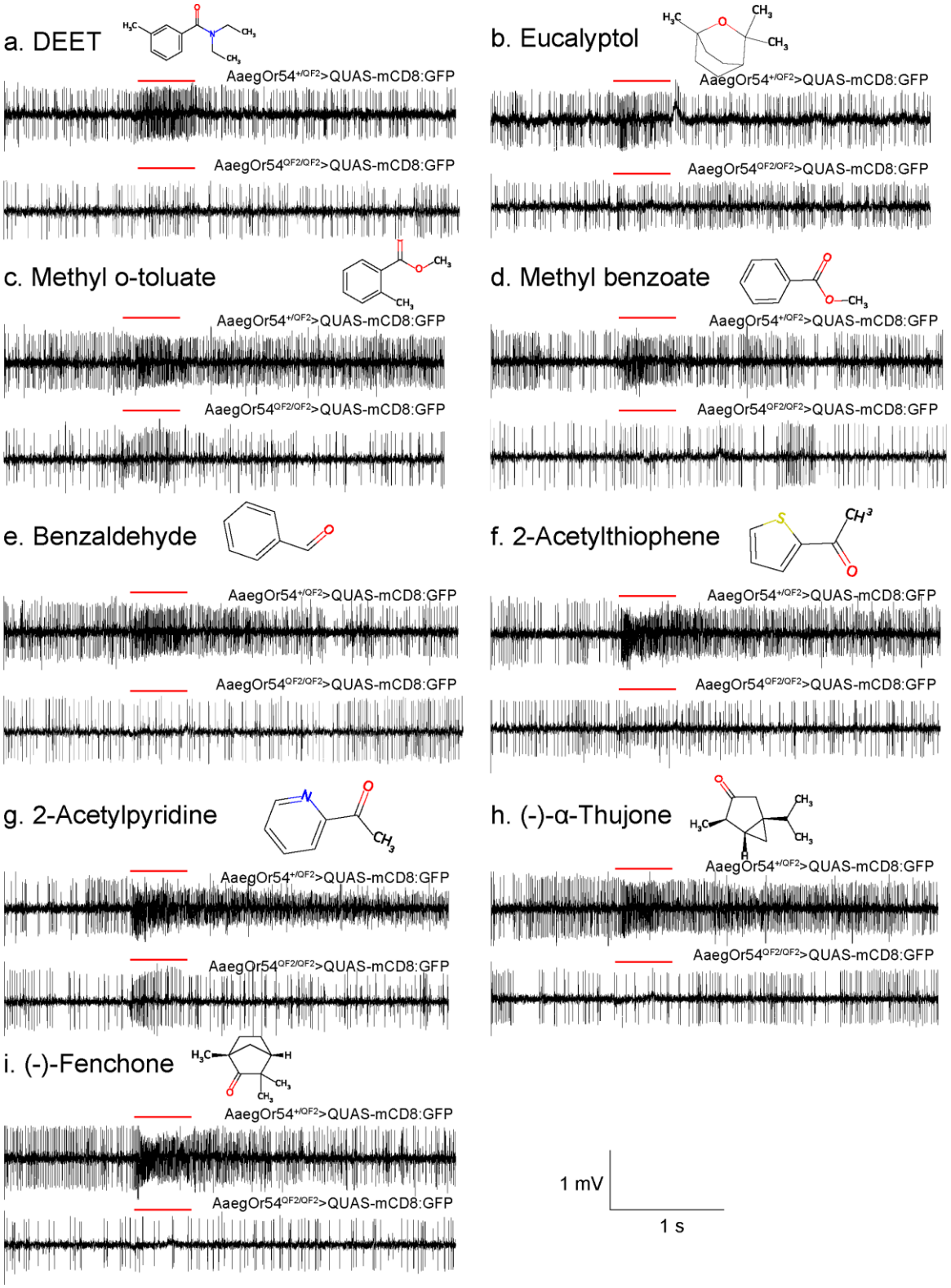

Fig. S6. Representative FgSSR traces from *AaegOr54*-expressing sensilla.
Representative odorant-evoked responses recorded from *AaegOr54*-expressing SST sensilla in heterozygous (*AaegOr54*$^{+/QF2}$ > *QUAS-mCD8:GFP*) and homozygous (*AaegOr54*$^{QF2/QF2}$ > *QUAS-mCD8:GFP*) mosquitoes. Responses to **(a)** DEET, **(b)** eucalyptol, **(c)** methyl o-toluate, **(d)** methyl benzoate, **(e)** benzaldehyde, **(f)** 2-

acetylthiophene, **(g)** 2-acetylpyridine, **(h)** (-)-α-thujone, and **(i)** (-)-fenchone are shown.

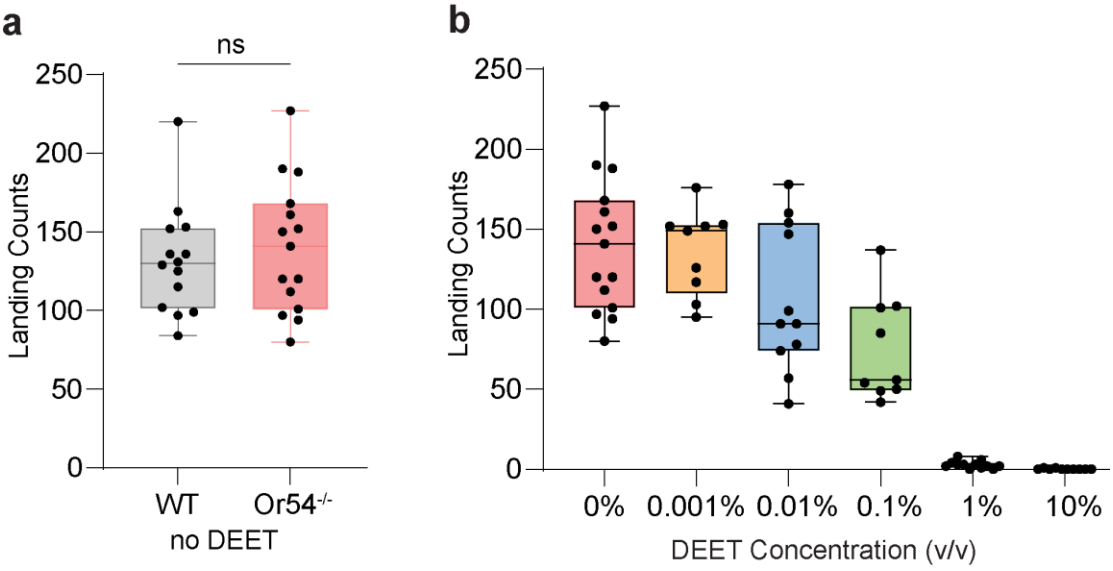

Fig. S7. Female *AaegOr54* mutants are less sensitive to DEET. a, Landing counts of WT and *AaegOr54*$^{-/-}$ mosquitoes in the absence of DEET, assessed using the hand-in-cage assay (n = 14-15, Mann-Whitney test; ns, not significant). **b,** Effect of DEET concentration on landing counts in *AaegOr54*$^{-/-}$ mosquitoes (n = 9-15).

Tables S1 to S5

Table S1. Transcription level of proximal part and distal part of antenna. Values are presented as Transcripts Per Million (TPM).

Vectorbase Identifier	Gene name	Proximal flagellomeres (1st-9th)			Distal flagellomeres (10th-13th)		
		1#	2#	3#	1#	2#	3#
AAEL006003	Or10	42.519957	48.434036	43.835042	16.89739	16.079155	21.696584
AAEL011409	Or100	30.853886	31.183472	26.121842	2.762648	3.611861	9.656852
AAEL017050	Or101	1.601759	0.973521	0.558299	0	0	0
AAEL023017	Or102	0.111459	1.25283	0.284456	0	0	0
AAEL017505	Or103	74.207979	57.040915	74.693258	0	0	1.971402
AAEL016966	Or104	21.09108	31.177808	35.628358	9.3291	16.317778	23.997413
AAEL019984	Or105	17.529422	27.313024	19.569427	18.608793	22.74269	20.358128
AAEL022439	Or107	1.229419	2.316561	0.487761	0.041439	0	0
AAEL018070	Or108	24.550382	34.55031	26.328332	0	0	0
AAEL011583	Or11	57.954556	65.482079	53.317584	64.129978	53.773472	55.664036
AAEL016983	Or110	5.903525	6.917759	13.521553	0	0.313382	0
AAEL024663	Or111	64.671407	82.227519	35.897007	54.07746	39.627936	53.310376
AAEL026829	Or112	74.178339	119.930992	66.535789	33.952905	58.687378	56.893589
AAEL017123	Or113	58.543959	42.291562	44.209985	38.151295	22.028645	43.376522
AAEL017219	Or114	17.186495	27.91063	8.148854	0	0	0
AAEL017361	Or115	18.442348	2.518555	18.142895	0	0	0.1561

AAEL025139	Or116	13.024107	12.861399	15.089517	0	0	0
AAEL017377	Or117	8.268929	4.46984	5.435997	0	0	0.571057
AAEL018107	Or118	4.007587	3.063586	1.33536	0	0	0
AAEL017009	Or119	2.626067	1.489589	3.571017	0	0.070838	0
AAEL017104	Or121	21.595388	17.601057	26.417171	0.066994	0	0.148769
AAEL013563	Or122	0.278892	0.675004	9.840987	0	0	0
AAEL017537	Or123	21.152573	21.253609	13.929717	0	0.743462	1.049402
AAEL013893	Or125	1.768132	12.972459	8.519073	0	0	0
AAEL008368	Or13	7.885558	8.118209	7.552106	0	0	0
AAEL010669	Or132	84.069011	83.968643	85.493968	98.008312	72.547283	84.527769
AAEL022696	Or133	3.596177	0.885094	2.181615	10.620224	11.651715	6.084959
AAEL008442	Or14	10.776184	11.237592	17.027646	16.952874	17.332973	16.183721
AAEL008448	Or15	4.379668	4.595396	4.81098	4.398111	7.77585	8.420259
AAEL007110	Or16	5.1817	1.346018	3.361195	64.489554	56.019165	42.18492
AAEL005999	Or2	41.336906	26.177998	41.800004	0.060872	9.09508	15.731008
AAEL025135	Or20	0	0	0	4.912806	16.916373	26.052273
AAEL017398	Or21	3.84233	3.345013	3.73862	43.780125	11.626573	18.656099
AAEL021097	Or22	2.711714	2.308809	0.806281	7.9391	13.453561	7.042364
AAEL001510	Or23	20.374974	14.494314	18.384089	19.456625	7.67917	7.89595
AAEL017557	Or24	5.234801	0	0.464602	34.429322	10.581584	21.055492
AAEL003629	Or25	0.221991	1.458031	0	28.309935	4.332465	12.923096
AAEL010428	Or26	36.735797	14.350762	22.532251	20.471254	13.321798	30.480514
AAEL010418	Or27	19.036547	16.011751	17.797389	74.879633	64.428596	97.172763
AAEL027053	Or28	4.132741	7.29695	4.604707	18.706537	12.425736	25.138376
AAEL022663	Or29	35.203956	24.164046	38.742821	2.702786	0.85283	0.227099
AAEL010409	Or30	5.036191	0.549613	2.218202	36.787288	48.574173	23.896847
AAEL013217	Or31	0	0	0.129782	44.06654	44.107516	49.958059
AAEL023626	Or32	7.767832	2.264384	4.354597	3.540125	3.009558	12.146217
AAEL017362	Or33	0	0.144548	0	7.958718	10.936858	6.89353
AAEL003395	Or34	1.787674	1.975865	2.71854	1.898118	1.708444	3.639511
AAEL016981	Or36	8.715433	8.565562	6.731705	8.355754	4.017164	3.390896
AAEL020435	Or37	1.8018	1.708632	1.701659	0.944058	1.441398	4.466741
AAEL005489	Or38	51.43408	51.012967	70.789334	0.320671	0	0
AAEL015147	Or4	105.907549	103.71533	102.103917	137.480425	76.766313	111.679833
AAEL003045	Or41	8.607749	3.461432	8.921876	22.061982	38.231791	28.520972
AAEL000616	Or42	1.522016	0.071315	1.16577	1.16221	5.937422	2.077543
AAEL017294	Or43	2.327413	1.310046	0.198262	8.367358	9.213612	5.391255
AAEL006465	Or44	5.390471	2.058954	1.771207	42.779675	24.023272	36.156871
AAEL000613	Or45	2.053126	1.564385	0.546379	25.312923	20.816809	24.382658
AAEL017079	Or47	53.59655	69.419248	61.223757	99.624919	64.012508	127.633257
AAEL020825	Or48	0.867646	0.567268	0.31696	0.373297	0.259248	0

AAEL010426	Or50	3.32819	5.193696	2.404213	17.653887	13.011453	18.503409
AAEL018080	Or51	5.276703	3.695085	5.093447	14.832841	26.724128	22.777232
AAEL013507	Or52	21.497034	18.642898	15.213825	7.39507	12.974361	6.930257
AAEL015286	Or54	0.248278	0	0.422908	25.68359	36.680545	41.651783
AAEL010415	Or55	0	0.116063	0	48.768198	37.668346	49.309785
AAEL027258	Or57	0	0	0.117552	2.607585	3.155483	1.803345
AAEL001342	Or59	30.465925	24.049809	42.960108	0	2.805619	0
AAEL017548	Or6	5.985996	2.06708	6.104397	33.738909	39.439437	41.201224
AAEL000628	Or63	5.410647	3.607426	1.310384	64.942789	57.404427	52.582181
AAEL000614	Or64	4.595981	5.482498	1.636963	55.612639	65.394832	99.222281
AAEL017227	Or66	0	0	0	0.12582	0	0
AAEL001221	Or69	29.029789	19.661665	22.595371	54.441654	44.729253	62.1732
AAEL026167	Or70	7.373551	7.269333	9.21689	13.385967	10.487171	7.763477
AAEL017564	Or71	15.507825	21.547977	14.040062	35.545124	24.310442	43.670332
AAEL017129	Or72	13.741332	13.595023	6.914704	8.594551	6.425981	9.415534
AAEL013418	Or76	0	1.095218	1.591424	0.876916	1.736938	1.017316
AAEL013422	Or77	2.103481	0.193323	1.228608	0.220273	0.420972	3.099583
AAEL013423	Or78	11.074172	9.327964	8.868783	10.619847	8.544367	19.107013
AAEL013420	Or79	62.221278	26.880435	49.060503	26.037745	21.388288	78.7681
AAEL012254	Or8	0	0.143607	0	0	0	0
AAEL017221	Or80	2.698282	1.073987	1.950253	2.508401	1.423277	4.444964
AAEL017305	Or81	5.292919	5.166776	7.161095	6.63495	5.265073	7.50724
AAEL026266	Or82	4.425141	3.717901	2.039762	18.029121	12.778124	11.04622
AAEL017043	Or84	354.026256	337.30365	263.628769	0.649102	9.250079	43.786247
AAEL004218	Or85	32.764468	27.737753	21.418044	0.412431	0.071535	0.533371
AAEL017246	Or86	8.714051	4.04442	5.033863	0	0	1.265734
AAEL017347	Or87	257.069359	236.697344	335.914379	40.876451	75.912416	146.198484
AAEL014197	Or88	23.473893	18.019226	12.243807	21.491198	19.627504	7.659892
AAEL017149	Or91	12.173119	16.73356	19.850639	0	0	0
AAEL017296	Or93	0.80144	0.666558	2.793444	0	0	0
AAEL017201	Or94	76.346778	53.179572	48.465069	0.162977	0.075367	6.903438
AAEL017427	Or96	10.875248	10.167399	11.273167	0	0.254429	0
AAEL027077	Or96	10.875248	10.167399	11.273167	0	0.254429	0
AAEL017236	Or99	0.996164	1.398813	1.429303	0	0	0

Table S2. Responses of *AaegOr54* against chemical compounds in TEVC system.

Compounds	***AaegOr54***		
	Mean	**SEM**	**n**
Acetic acid	13.33	6.67	3
Myristic acid	10.00	0.00	3
Hexanoic acid	3.33	3.33	3
Heptanoic acid	3.33	3.33	3

Propionic acid	3.33	3.33	3
Heptadecanoic acid	6.67	3.33	3
(*L*)-(+)-Lactic acid	0.00	3.65	6
n-Pentadecanoic acid	-1.67	3.07	6
Benzoic acid	-5.00	4.28	6
trans-23-Dimethylacrylic acid	-1.67	3.07	6
(d/l)-3-Methylvaleric acid	-1.67	9.10	6
Octanoic acid	-8.33	6.01	6
Decanoic acid	-13.33	5.58	6
Undecanoic acid	-12.00	5.83	5
Lauric acid	-5.71	2.97	7
n-Tridecanoic acid	-5.00	2.24	6
Adipic acid	1.67	4.01	6
Pimelic acid	-1.67	3.07	6
4-Hydroxybenzoic acid	1.67	1.67	6
Acrylic acid	-1.67	1.67	6
n-Nonanoic acid	-1.67	4.77	6
Oleic acid	3.33	6.67	3
Palmitic acid	-22.00	3.74	5
Hexanal	22.86	2.86	7
Propanal	-13.33	6.67	3
Decanal	10.00	3.78	7
Nonanal	11.43	4.04	7
Benzaldehyde	24.29	7.82	7
Heptanal	17.14	8.65	7
Pentanal	18.57	3.40	7
Octanal	30.00	7.56	7
Butanal	32.86	12.29	7
Isobutanal	22.86	2.86	7
2-Methylbutanal	15.71	5.28	7
Citronellal	15.71	2.02	7
(*S*)-(−)-Perillaldehyde	-12.86	2.86	7
Citral	2.50	2.50	4
2-Decanol	-16.67	3.33	3
Phenol	0.00	15.28	3
trans-2-Hexen-1-ol	14.29	2.97	7
1-Tetradecanol	0.00	5.77	3
2-Hexadecanol	10.00	5.77	3
cis-2-Hexen-1-ol	22.86	4.21	7
Glycerol	-6.67	3.33	3
1-Hexen-3-ol	3.33	6.67	3
1-Octen-3-ol	0.00	5.77	3
trans-2-Octen-1-ol	7.14	5.22	7

4-Ethyl phenol	0.00	10.00	3
p-Cresol	28.57	5.95	7
Phenelethyl alcohol	-6.67	3.33	3
Isoamyl alcohol	-23.33	8.82	3
Cinnamyl alcohol	13.33	17.64	3
(*S*)-(−)-Perilly alcohol	-5.00	2.89	4
α-Terpineol	2.86	1.84	7
(+)-Terpinen-4-ol	5.00	2.89	4
d-Neomethol	5.00	2.89	4
Menthol	-12.50	6.29	4
Geraniol	0.00	7.07	4
Citronellol	-4.29	3.69	7
(*S*)-cis-Verbenol	4.29	2.97	7
Linalool	2.50	4.79	4
n-Heptadecane	-6.67	3.33	3
Toluene	5.71	4.81	7
1-Hexadecene	0.00	0.00	3
1-Tetradecene	3.33	3.33	3
n-Nonane	-6.67	3.33	3
Benzene	30.00	4.88	7
Squalene	-3.33	3.33	3
Propylbenzene	3.33	6.67	3
n-Pentadecane	3.33	3.33	3
Hexadecane	36.00	11.22	5
trans-2-Octene	10.00	0.00	3
n-Octadecane	3.33	3.33	3
Styrene	13.33	3.33	3
n-Decane	-6.67	3.33	3
Xylene	90.00	41.06	7
Ethylbenzene	8.57	5.08	7
2,4-Dimethylhexane	16.67	3.33	3
trans-4-Octene	13.33	6.67	3
trans-3-Octene	13.33	6.67	3
n-Octane	0.00	0.00	3
2-Pentene	3.33	3.33	3
Hexane	-3.33	3.33	3
Heptane anhydrous	0.00	5.77	3
Thymol	15.00	2.89	4
Carvacrol	10.00	0.00	3
Methyl nonanoate	6.67	8.82	3
Methyl tridecanoate	3.33	6.67	3
Dimethyl phthalate	308.33	38.59	6
Dibutyl phthalate	21.67	1.67	6

Menthyl acetate	111.43	17.52	7
Linalyl acetate	30.00	9.76	7
2-Hexanone	32.86	6.44	7
2-Pentanone	-6.67	3.33	3
3-Pentanone	3.33	3.33	3
2-Decanone	3.33	8.82	3
2-Butanone	17.14	4.74	7
Sulcatone	51.43	14.55	7
(−)-Menthone	55.71	11.31	7
(+)-Menthone	25.00	4.28	6
Geranyl acetone	-7.50	4.79	4
Camphor	15.71	7.19	7
(−)-α-Thujone	50.00	10.00	7
Propylamine	0.00	5.77	3
Butylamine	-3.33	3.33	6
Ammonia	2.00	2.00	5
Carbon disulfide	-2.00	2.00	5
Methyl disulfide	2.00	3.74	5
Urea	10.00	5.77	3
Methylurea	-3.33	6.67	3
Thiourea	135.00	21.41	6
1-Chloroheptane	1.67	4.77	6
Lauryl chloride	421.67	80.31	6
1-Chlorotetradecane	146.00	16.00	5
1-Chlorohexadecane	-11.43	3.40	7
1-Chlorohexane	15.00	22.02	6
Benzyl chloride	-4.29	4.81	7
Indole	8.00	10.68	5
3-Aminopyridine	-3.33	2.11	6
4-Aminopyridine	6.67	3.33	3
1-Methylpiperazine	10.00	0.00	3
2-Methylfuran	-20.00	10.00	2
Thiazolidine	23.33	3.33	3
2,6-Dimethylpyrazine	-4.29	4.81	7
Skatole	-10.00	17.32	3
Coumarin	33.33	79.65	3
n-Piperidineethanol	-30.00	20.00	2
4-Peridinemethanamine	5.00	2.24	6
Pyrazine	28.57	5.95	7
(*R*)-(+)-Limonene	6.67	3.33	3
(*S*)-(−)-Limonene	0.00	0.00	3
α-Terpinene	18.57	9.86	7
Myrcene	0.00	0.00	3

α-Pinene	10.00	0.00	4
(+)-α-Pinene	5.00	2.89	4
(−)-α-Pinene	5.00	2.89	4
(−)-β-Pinene	0.00	3.16	5
(+)-β-Pinene	10.00	0.00	4
(+)-3-Carene	5.00	2.89	4
Eugenol	126.67	21.55	6
Terpenolene	24.29	6.12	7
Eucalyptol	22.86	5.22	7
β-Caryophyllene	2.86	2.86	7
(−)-Caryophyllene oxide	5.00	2.89	4
Phytol	4.00	2.45	5
DEET	1462.00	155.09	5
Permethrin	7.50	2.50	4
Naphthalene	14.00	2.45	5
β-Cypermethrin	3.33	3.33	3
Deltamethrin	6.67	3.33	3
IR3535	-3.33	6.67	3
Picaridin	-13.33	6.67	3
Mehyl salicylate	0.00	5.77	3
(+)-Fenchone	-13.33	3.33	3
Methyl dihydrojasmolate	3.33	6.67	3
Methyl jasmonate	0.00	5.77	3
PMD	-3.33	3.33	3

Table S3. Response profiles of *AaegOr54* in *Drosophila* empty neuron expression system.

Compound	Responses			Mean	SEM
	1#	2#	3#		
Amylacetate	-5	-8	-12	-8.33	2.03
trans-2-Octen-1-ol	-5	0	-12	-5.67	3.48
DMSO	3	-8	-12	-5.67	4.48
Geraniol	-11	-4	0	-5.00	3.21
Citronellic acid	-7	-2	-4	-4.33	1.45
2,3-Butanedione	-7	2	-6	-3.67	2.85
α-Terpineol	-5	-2	-2	-3.00	1.00
Phenol	-3	-6	0	-3.00	1.73
2-Decanol	-3	-6	0	-3.00	1.73
Furfural	-9	8	-4	-1.67	5.04
2-Propylphenol	-1	-2	-2	-1.67	0.33
2-Picoline	-3	2	-4	-1.67	1.86
Methanol	1	0	-6	-1.67	2.19
1-Pentanol	-5	-2	2	-1.67	2.03

Ethyl propanoate	5	2	-12	-1.67	5.24
Methyl hexanoate	1	0	-6	-1.67	2.19
Hexyl hexanoate	-7	6	-4	-1.67	3.93
Decanoic acid	3	2	-10	-1.67	4.18
Terpinolene	-5	0	2	-1.00	2.08
Methyl disulfide	1	0	-4	-1.00	1.53
2-Methylphenol	1	0	-4	-1.00	1.53
1-Hexanol	1	6	-10	-1.00	4.73
1-Penten-3-ol	-1	-2	0	-1.00	0.58
1-Hexen-3-ol	-7	8	-4	-1.00	4.58
Ethyl hexanoate	-3	2	0	-0.33	1.45
Ethyl benzene	-5	4	2	0.33	2.73
Styrene	-9	2	8	0.33	4.98
Xylene	-5	-2	8	0.33	3.93
Indole	1	8	-8	0.33	4.63
Skatole	-5	0	6	0.33	3.18
4-Methylthiazole	-1	2	0	0.33	0.88
3-Methyl-2-buten-1-ol	-1	-4	6	0.33	2.96
1-Octen-3-ol	-9	16	-6	0.33	7.88
Cinnamyl alcohol	5	0	-4	0.33	2.60
(*E*)-3-Hexenol	-3	2	2	0.33	1.67
Isopentyl acetate	-5	2	4	0.33	2.73
Ethyl propionate	7	-2	-4	0.33	3.38
Ethyl octanoate	3	0	-2	0.33	1.45
trans-3-Octene	-3	0	4	0.33	2.03
Hexanal	3	0	-2	0.33	1.45
Nonanal	1	2	-2	0.33	1.20
α-(-)-Thujone	-5	0	6	0.33	3.18
Butanoic acid	1	6	-6	0.33	3.48
(*Z*)-2-Hexenol	-3	2	4	1.00	2.08
Hexyl acetate	-5	4	4	1.00	3.00
ethyl-3-Hydroxybutyrate	-1	10	-6	1.00	4.73
Propional	-5	6	2	1.00	3.21
Acetaldehyde	1	8	-6	1.00	4.04
Undecanoic acid	-3	2	4	1.00	2.08
β-Mycrene	-3	12	-2	2.33	4.84
Limonene	-5	-2	14	2.33	5.90
Eugenol	-1	8	0	2.33	2.85
(-)-Linalool	-13	6	14	2.33	8.01
(-)-Menthone	1	4	2	2.33	0.88
3-methylthio-1-propanol	1	6	0	2.33	1.86
Benzyl alcohol	1	10	-4	2.33	4.10
2-Ethyl toluene	-3	2	8	2.33	3.18

2-Methyl furan	5	4	-2	2.33	2.19
Ethyl formate	-5	8	4	2.33	3.84
Methyl nonanoate	3	-2	6	2.33	2.33
trans-4-Octene	-3	4	6	2.33	2.73
trans-Cinnamaldehyde	1	4	2	2.33	0.88
Heptanal	5	6	-4	2.33	3.18
α-Terpinene	-1	8	2	3.00	2.65
Eucalyptol	-5	12	2	3.00	4.93
Benzyl methyl ether	3	12	-6	3.00	5.20
Benzyl acetate	3	12	-6	3.00	5.20
3-Methylphenol	5	0	4	3.00	1.53
4-Methylphenol	-3	10	2	3.00	3.79
2-Pentanol	3	4	2	3.00	0.58
(E)-2-Hexenyl acetate	-3	0	14	3.67	5.24
Ethyl butyrate	-5	6	10	3.67	4.48
Dodecanoic acid	-1	4	8	3.67	2.60
Pentanoic acid	-7	10	8	3.67	5.36
(*S*)-(-)-Perillaldehyde	5	4	4	4.33	0.33
6-Methyl-5-hepten-2-one	3	14	-4	4.33	5.24
Methyl acetate	-7	12	8	4.33	5.78
Menthol	-1	6	10	5.00	3.21
Citronellal	9	6	0	5.00	2.65
(+)-Terpinen-4-ol	-5	20	0	5.00	7.64
Dimethylsulfide	5	2	10	5.67	2.33
Thiazole	5	6	6	5.67	0.33
γ-Hexalactone	1	12	8	7.00	3.21
Benzene	3	12	6	7.00	2.65
3-Octanone	5	18	2	8.33	4.91
4,5-Dimethylthiazole	11	14	0	8.33	4.26
Methyl octanoate	-3	14	14	8.33	5.67
2-Acetylthiazole	11	14	8	11.00	1.73
2,4,5-Trimethylthiazole	11	22	10	14.33	3.84
1-Indanone	9	24	20	17.67	4.48
Methyl-2-methyl-benzoate	23	40	6	23.00	9.81
2-Acetylthiophene	25	40	28	31.00	4.58
DEET	21	40	46	35.67	7.54
Acetophenone	15	44	18	25.67	9.21
2-Acetylpyridine	5	28	24	19.00	7.09
Naphthalene	7	28	16	17.00	6.08
2-Isobutylthiazole	9	24	4	12.33	6.01
Methyl benzoate	13	16	4	11.00	3.61
Propylbenzene	7	10	14	10.33	2.03
β-Caryophyllene	5	8	12	8.33	2.03

Carbon disulfide	1	10	12	7.67	3.38
Neomenthol	5	8	10	7.67	1.45
2-Ethoxythiazole	1	12	6	6.33	3.18
Hexyl butyrate	-3	10	12	6.33	4.70
Geranyl acetate	-7	6	18	5.67	7.22
4-Methylcyclohexanol	-1	12	4	5.00	3.79
Pentyl acetate	3	6	6	5.00	1.00
Ethyl lactate	3	14	-2	5.00	4.73
(L)-(+)-lactic acid	3	6	6	5.00	1.00
Methyl acetate	-7	12	8	4.33	5.78
(-)-Fenchone	1	8	2	3.67	2.19
Linalyl acetate	-3	6	8	3.67	3.38
2-Hexanone	5	10	-4	3.67	4.10
Benzaldehyde	-1	2	10	3.67	3.28
2,6-Dimethylpyrazine	-9	6	14	3.67	6.74
1-Heptanol	1	4	6	3.67	1.45
1-Hepten-3-ol	3	8	0	3.67	2.33
(E)-2-hexenol	1	4	4	3.00	1.00
Dimethyl phthalate	7	4	-2	3.00	2.65
Pentanal	-1	6	4	3.00	2.08
Octanal	-5	8	6	3.00	4.04
Decanal	-1	12	-2	3.00	4.51
(*S*)-(-)-Limonene	-5	6	4	1.67	3.38
Citronellol	-1	0	6	1.67	2.19
(-)-Carvone	3	0	2	1.67	0.88
(+)-Fenchone	-7	2	10	1.67	4.91
Linalool oxide	3	-2	4	1.67	1.86
Linalool	5	-4	4	1.67	2.85
2-Nonanone	9	-4	0	1.67	3.84
Phenethyl acetate	-3	-2	10	1.67	4.18
Methyl salicylate	9	14	-18	1.67	9.94
Phenylacetaldehyde	-7	-2	14	1.67	6.33
Coumarin	-5	4	6	1.67	3.38
3-Methyl-1-butanol	3	6	-4	1.67	2.96
2,3-Butanediol	-3	10	-2	1.67	4.18
Ethyl methanoate	-3	8	0	1.67	3.28
Ammonia	-5	10	0	1.67	4.41
α-Pinene	-7	6	4	1.00	4.04
Nerol	-5	6	2	1.00	3.21
2-Heptanone	1	6	-4	1.00	2.89
Cyclohexanone	-5	10	-2	1.00	4.58
Ethyl cinnamate	-3	-4	10	1.00	4.51
4-Ethylphenol	-5	-2	10	1.00	4.58

1-Dodecanol	1	4	-2	1.00	1.73
(*R*)-(+)-Limonene	-11	6	4	-0.33	5.36
3-Carene	-1	8	-8	-0.33	4.63
(-)-α-Pinene	-3	10	-8	-0.33	5.36
(-)-β-Pinene	-5	4	0	-0.33	2.60
Citral	-7	8	-2	-0.33	4.41
2-Decanone	-1	4	-4	-0.33	2.33
Phenethyl alcohol	1	0	-2	-0.33	0.88
Ethyl benzoate	-5	8	-4	-0.33	4.18
1-Butanol	-1	-2	2	-0.33	1.20
Propyl acetate	-5	2	2	-0.33	2.33
Methyl propanoate	1	2	-4	-0.33	1.86
Ethyl hexanoate	-3	2	0	-0.33	1.45
trans-2-Octene	-5	4	0	-0.33	2.60
Tridecanoic acid	1	0	-2	-0.33	0.88
(+)-Pulegone	-3	8	-6	-0.33	4.26
(1*S*)-(+)-3-Carene	-7	4	4	0.33	3.67
(+)-α-Pinene	-5	6	0	0.33	3.18
Geranyl acetone	-1	0	2	0.33	0.88
o-Cresol	-5	4	2	0.33	2.73
Butyl acetate	-5	4	-2	-1.00	2.65
Isoamyl acetate	3	-2	-4	-1.00	2.08
Methyl butylate	3	2	-8	-1.00	3.51
Isobutanal	-1	0	-2	-1.00	0.58
2-Methylbutanal	-3	10	-10	-1.00	5.86
Pyruvic acid	-5	4	-2	-1.00	2.65
Paraffin oil	1	-4	0	-1.00	1.53
(*S*)-cis-Verbenol	-9	6	-2	-1.67	4.33
2-Pentanone	-5	6	-6	-1.67	3.84
3-Pentanone	1	0	-6	-1.67	2.19
Thymol	-7	0	0	-2.33	2.33
(+)-Carvone	-9	6	-4	-2.33	4.41
Menthyl acetate	-13	10	-4	-2.33	6.69
Estragole	-7	6	-6	-2.33	4.18
1-Octanol	-1	4	-10	-2.33	4.10
2-Ethyl-1-hexanol	-1	-2	-4	-2.33	0.88
Hexanoic acid	-1	2	-8	-2.33	2.96
Ethyl trans-2-butenoate	-1	-2	-6	-3.00	1.53
Butanal	-3	2	-8	-3.00	2.89
Linoleic acid	-7	8	-10	-3.00	5.57
2-Ethylphenol	-3	-6	-2	-3.67	1.20
1-Propanol	-1	0	-10	-3.67	3.18
Isobutyl acetate	-3	8	-16	-3.67	6.94

γ-Octalactone	-5	4	-18	-6.33	6.39
Camphor	-17	0	-6	-7.67	4.98

1183

1184 **Table S4**. Sequencing of the mutants. The genomic sequence, inserted sequence, and
1185 stop codon are shown in black, red, and green, respectively.

Mutant	Sequence
AaegOr54$^{-/-}$	GATAATCCAATTACCATCCGCGTTATTTAAAGATAATTGCGTTTTTATTGTCAGGGA GTGAGTTTGCTTAAAAACTCGTTTAGATCCAATTCGAGCTCGCCCGGGGATCTAATT CAATTAGAGACTAATTCAATTAGAGCTAATTCAATTAGGATCCAAGCTTATCGATTTC GAACCCTCGACCGCCGGAGTATAAATAGAGGCGCTTCGTCTACGGAGCGACAATTC AATTCAAACAAGCAAAGTGAACACGTCGCTAAGCGAAAGCTAAGCAAATAAACAA GCGCAGCTGAACAAGCTAAACAATCGGGGTACCGCTAGAGTCGACGGTACCGCGG GCCCGGGATCCACCGGTCGCCACCATGGCCTCCTCCGAGAACGTCATCACCGAGTT CATGCGCTTCAAGGTGCGCATGGAGGGCACCGTGAACGGCCACGAGTTCGAGATCG AGGGCGAGGGCGAGGGCCGCCCCTACGAGGGCCACAACACCGTGAAGCTGAAGGT GACCAAGGGCGGCCCCCTGCCCTTCGCCTGGGACATCCTGTCCCCCCAGTTCCAGT ACGGCTCCAAGGTGTACGTGAAGCACCCCGCCGACATCCCCGACTACAAGAAGCTG TCCTTCCCCGAGGGCTTCAAGTGGGAGCGCGTGATGAACTTCGAGGACGGCGGCGT GGCGACCGTGACCCAGGACTCCTCCCTGCAGGACGGCTGCTTCATCTACAAGGTGA AGTTCATCGGCGTGAACTTCCCCTCCGACGGCCCCGTGATGCAGAAGAAGACCATG GGCTGGGAGGCCTCCACCGAGCGCCTGTACCCCCGCGACGGCGTGCTGAAGGGCG AGACCCACAAGGCCCTGAAGCTGAAGGACGGCGGCCACTACCTGGTGGAGTTCAA GTCCATCTACATGGCCAAGAAGCCCGTGCAGCTGCCCGGCTACTACTACGTGGACG CCAAGCTGGACATCACCTCCCACAACGAGGACTACACCATCGTGGAGCAGTACGAG CGCACCGAGGGCCGCCACCACCTGTTCCTGTAGCGGCCGCGACTCTAGATCATAATC AGCCATACCACATTTGTAGAGGTTTTACTTGCTTTAAAAAACCTCCCACACCTCCCC CTGAACCTGAAACATAAAATGAATGCAATTGTTGTTGTTAACTTGTTTATTGCAGCTT ATAATGGTTACAAATAAAGCAATAGCATCACAAATTTCACAAATAAAGCATTTTTTTC ACTGCATTCTAGTTGTGGTTTGTCCAAACTCATCAATGTATCTTATAATGGATGCAGA GTGAGTCACC
AaegOr54-QF	GATAATCCAATTACCATCCGCGGAGGGCAGAGGAAGTCTTCTAACATGCGGTGAC GTGGAGGAGAATCCCGGCCCTATGCCACCCAAGCGCAAAACGCTTAACGCTGCGGC TGAGGCTAACGCTCATGCCGACGGACACGCCGACGGAAACGCCGACGGACACGTG GCCAATACGGCCGCGTCCTCGAATAATGCGAGGTTCGCTGATCTCACTAACATCGAT ACTCCGGGTCTGGGACCCACAACTACGACCCTGCTCGTGGAACCAGCACGCTCAAA GCGTCAACGAGTGTCCCGCGCATGCGACCAGTGCCGTGCAGCCCGAGAGAAATGC GACGGAATACAGCCTGCGTGTTTCCCGTGCGTTTCCCAGGGAAGGTCCTGCACTTAT CAGGCTTCGCCGAAAAAGAGGGGAGTTCAAACCGGTTATATTCGTACGCTGGAGCT CGCCCTCGCCTGGATGTTTGAAAATGTCGCGCGTTCCGAAGATGCCTTGCATAACCT CCTCGTCCGTGACGCCGGACAAGGATCAGCTCTGCTCGTTGGTAAAGATTCGCCGG CTGCCGAGCGACTCCATGCCCGTTGGGCTACTAGCCGTGTCAATAAGAGCATTACCC

	GCCTCCTCCGTCAGTTGGAGCTCCCTCCTACCGCCACGGCTACGGCCTCGATAATGC CGCACGTGATGGAGCAGCCTCTCAGTACCAGCATTAACCCCGTCAACGACCGCTTC AACGGTATTCCCAACCCCACTCCGTATAACTCCGATGCAGCTCTCGATGCTATCACTC AGACCAACGATTATGGAAGCGTAAATACACATGGTATCCTCTCTACTTACCCGCCAC CGGCTACGCACCTTAATGAAGCTTCCGTCGCTCTCGCTCCCGGTGGCGCCCCCCCCC GACCGCCTCCTCCGTATGTTGACAGCACGACCAATCACCCGCCGTACCACTCGAATC TGGTTCCAATGGCGAACTTTGGTTACTCGACCGTTGATTACGATGCCATGGTTGACG ATTTGGCTAGCATTGAATACACGGACGCTGTGGATGTCGACCCACAGTTTATGACCA ATCTGGGATTCGTTCCTGGATGTAACTTCTCCGACATTAATACATACGAACAGTGATG ACGTCTATCGATACCGTCGACTAAAGCCAAATAGAAAATTATTCAGTTCCTGGCTTAA GTTTTTAAAAGTGATATTATTTATTTGGTTGTAACCAACCAAAAGAATGTAAATAACT AATACATAATTATGTTAGTTTTAAGTTAGCAACAAATTGATTTTAGCTATATTAGCTAC TTGGTTAATAAATAGAATATATTTATTTAAAGATAATTGCGTTTTTATTGTCAGGGAGT GAGTTTGCTTAAAAACTCGTTTAGATCCAATTCGAGCTCGCCCGGGGATCTAATTCA ATTAGAGACTAATTCAATTAGAGCTAATTCAATTAGGATCCAAGCTTATCGATTTCGA ACCCTCGACCGCCGGAGTATAAATAGAGGCGCTTCGTCTACGGAGCGACAATTCAAT TCAAACAAGCAAAGTGAACACGTCGCTAAGCGAAAGCTAAGCAAATAAACAAGCG CAGCTGAACAAGCTAAACAATCGGGGTACCGCTAGAGTCGACGGTACCGCGGGCCC GGGATCCACCGGTCGCCACCATGGCCTCCTCCGAGAACGTCATCACCGAGTTCATG CGCTTCAAGGTGCGCATGGAGGGCACCGTGAACGGCCACGAGTTCGAGATCGAGG GCGAGGGCGAGGGCCGCCCCTACGAGGGCCACAACACCGTGAAGCTGAAGGTGAC CAAGGGCGGCCCCCTGCCCTTCGCCTGGGACATCCTGTCCCCCCAGTTCCAGTACG GCTCCAAGGTGTACGTGAAGCACCCCGCCGACATCCCCGACTACAAGAAGCTGTCC TTCCCCGAGGGCTTCAAGTGGGAGCGCGTGATGAACTTCGAGGACGGCGGCGTGG CGACCGTGACCCAGGACTCCTCCCTGCAGGACGGCTGCTTCATCTACAAGGTGAAG TTCATCGGCGTGAACTTCCCCTCCGACGGCCCCGTGATGCAGAAGAAGACCATGGG CTGGGAGGCCTCCACCGAGCGCCTGTACCCCCGCGACGGCGTGCTGAAGGGCGAG ACCCACAAGGCCCTGAAGCTGAAGGACGGCGGCCACTACCTGGTGGAGTTCAAGT CCATCTACATGGCCAAGAAGCCCGTGCAGCTGCCCGGCTACTACTACGTGGACGCC AAGCTGGACATCACCTCCCACAACGAGGACTACACCATCGTGGAGCAGTACGAGCG CACCGAGGGCCGCCACCACCTGTTCCTGTAGCGGCCGCGACTCTAGATCATAATCAG CCATACCACATTTGTAGAGGTTTTACTTGCTTTAAAAAACCTCCCACACCTCCCCCTG AACCTGAAACATAAAATGAATGCAATTGTTGTTGTTAACTTGTTTATTGCAGCTTATA ATGGTTACAAATAAAGCAATAGCATCACAAATTTCACAAATAAAGCATTTTTTTCACT GCATTCTAGTTGTGGTTTGTCCAAACTCATCAATGTATCTTATAATGGATGCAGAGTG AGTCACC
AaegOr55$^{-/-}$	GGATTGGTTCCCGCTATTTTAACCAACCCGGTGCTAGGCAGCCATGTTTTCGTGGTC AGCATCAAACTCAAGAGCAATAACGTACATTGGCTTAATCATATAAAGGAATTTTTCC TCCTATACTAAAATGTGTTTCTAGCTAATCACATCAACCCAAATTGACTTGCTGTATT GCAATCCAATATTTTGTAACCGTTTATTTGTTCGAATAACTGTTGTTTTTACGGAAAA ATATTTTTTTCGGAGAAAAAGATTTCGCCATCATCGATTGTTATTCCGCAAACGGTTA TTTGTTTACAAACATTGAGCTGTCAGTGGGAACCACTTCCCAGTGGGAACCAGAGA

	TGTTTGCTCGTTATTTTTCAATGGGGTTGTATGGGCGGTGTCAGGAGGCTGATTTTAA CGACATACCGGTACTGTAACTCC

1186

1187 **Table S5**. Primers used in the project.

Primer name	Sequence
pT7Ts-AaegOr55F	GCAGATCTGATATCGCCACCATGCAGCAAAAACCTCCG
pT7Ts-AaegOr55R	GGGGTACCGGGCCCACTAGTCTATTCTCCGTAGAACTGCT
pT7Ts-AaegOr31F	GCAGATCTGATATCGCCACCATGGCGCCCACCCAAAATG
pT7Ts-AaegOr31R	GGGGTACCGGGCCCACTAGTTTAATTATCAGTGAATGATAAAAGCAAAGC
pT7Ts-AaegOr54F	GCAGATCTGATATCGCCACCATGAATACTAATTCACAA
pT7Ts-AaegOr54R	GGGGTACCGGGCCCACTAGTTCACTTATCTCCATAGAATT
pT7Ts-AaegOr57F	GCAGATCTGATATCGCCACCATGGTCGTAATCGCATCGATG
pT7Ts-AaegOr57R	GGGGTACCGGGCCCACTAGTCTACTCTTCTCCGTAGAACCG
pT7Ts-AaegOr20F	GCAGATCTGATATCGCCACCATGGATTTGCTGAACAAACTACAG
pT7Ts-AaegOr20R	GGGGTACCGGGCCCACTAGTTCAATCCTTTACACGCAAGAGC
pT7Ts-AaegOr25F	GCAGATCTGATATCGCCACCATGGAGGATGCAAAATTCGG
pT7Ts-AaegOr25F	GGGGTACCGGGCCCACTAGTCTATGAATTTTGTTTTTTGCTTAGTATGG
pT7Ts-AaegOr33F	GCAGATCTGATATCGCCACCATGGAACAGCACTTGAAGAAAATC
pT7Ts-AaegOr33F	GGGGTACCGGGCCCACTAGTTTATTTGCTAACCGTTCTAAACAAAG
pUASTattBBackboneF	GAATTCGTTAACAGATCTGCG
pUASTattBBackboneR	GAATTCCCAATTCCCTATTCA
pUASTattB-AaegOr54F	TGAATAGGGAATTGGGAATTCATGAATACTAATTCACAACCTCCG
pUASTattB-AaegOr54R	CGCAGATCTGTTAACGAATTCTCACTTATCTCCATAGAATTGCTGC
AaegOr54gRNA	TCACTCTGCATCCATTACCGCGG
AaegOr54ExamF	CCATCGTATTTGTTCAAGCTGG
AaegOr54ExamR	CACGGTATGGCCGAACAGTAC
AaegOr55gRNA	ATTACCTTCAGCGGTTATGGAGG
AaegOr55ExamF	GATCTACGTATCCATCGTATTC
AaegOr55ExamR	GCAACCATATCCAGTAATTGG
HDR-AaegOr54LAF	GTTGTAAAACGACGGCCAGTTTCGGCTAAGATCCTATCCCTG
HDR-AaegOr54LAR	GAAGACTTCCTCTGCCCTCCGCGGATGGTAATTGGATTATC
HDR-AaegOr54RAF	CTCATCAATGTATCTTATAATGGATGCAGAGTGAGTCACC
HDR-AaegOr54RAR	CACAGGAAACAGCTATGACCTTTCATTCATATCTCACAAAG
HDR-(T2A-QF-DsRed)F	GTCATAGCTGTTTCCTGTGTG
HDR-(T2A-QF-DsRed)R	ACTGGCCGTCGTTTTACAAC
HDR-(AmpR)F	GAGGGCAGAGGAAGTCTTC
HDR-(AmpR)R	TAAGATACATTGATGAGTTTGGACAAACC

1188

1189